Title

Host engulfment pathway controls inflammation in inflammatory bowel disease

Journal

The FEBS Journal, 287(18)

ISSN

1742-464X

Authors

Sayed, Ibrahim M

Suarez, Katherine

Lim, Eileen

et al.

Publication Date

2020-09-01

DOI

10.1111/febs.15236

Peer reviewed

HHS Public Access

Author manuscript

FEBS J. Author manuscript; available in PMC 2020 December 09.

Published in final edited form as:

FEBS J. 2020 September ; 287(18): 3967–3988. doi:10.1111/febs.15236.

Host engulfment pathway controls inflammation in Inflammatory Bowel Disease

Ibrahim M Sayed[1,*,$], **Katherine Suarez**[1,*], **Eileen Lim**[1,*], **Sujay Singh**[1,*], **Matheus Pereira**[1], **Stella-Rita Ibeawuchi**[1], **Gajanan Katkar**[3], **Ying Dunkel**[2], **Yash Mittal**[2], **Ranajoy Chattopadhyay**[3], **Monica Guma**[2], **Brigid S. Boland**[2], **Parambir S. Dulai**[2], **William J. Sandborn**[2], **Pradipta Ghosh**[2,3], **Soumita Das**[1]

[1]Department of Pathology, University of California San Diego; San Diego, USA

[2]Department of Medicine, University of California San Diego; San Diego, USA

[3]Department of Cellular & Molecular Medicine, University of California San Diego; San Diego, USA

Abstract

Chronic diseases, including inflammatory bowel disease (IBD) urgently need new biomarkers as a significant proportion of patients, do not respond to current medications. Inflammation is a common factor in these diseases and microbial sensing in the intestinal tract is critical to initiate the inflammation. We have identified ELMO1 (Engulfment and Cell Motility Protein-1) as a microbial sensor in epithelial and phagocytic cells that turns on inflammatory signals. Using a stem-cell-based “gut-in-a-dish” coculture model, we studied the interactions between microbes, epithelium and monocytes in the context of IBD. To mimic the *in-vivo* cell physiology, enteroid-derived monolayers (EDMs) were generated from the organoids isolated from WT and ELMO1−/− mice and colonic biopsies of IBD patients. The EDMs were infected with the IBD-associated microbes to monitor the inflammatory responses. ELMO1-depleted EDMs displayed a significant reduction in bacterial internalization, a decrease in pro-inflammatory cytokine productions and monocyte recruitment. The expression of ELMO1 is elevated in the colonic epithelium and in the inflammatory infiltrates within the lamina propria of IBD patients where the higher expression is positively correlated with the elevated expression of pro-inflammatory cytokines, MCP-1 and TNF-α. MCP-1 is released from the epithelium and recruits monocytes to the site of inflammation.

Address correspondence to Soumita Das, Department of Pathology, University of California, San Diego, 9500 Gilman Drive, MC 0644, San Diego, CA, 92093-0644, USA, Phone 858-246-2062, sodas@ucsd.edu.

Author Contributions: Study concept and design: IMS, RC, PG, SD
Acquisition of data: IMS, KS, EL, SS, MP, LPJ, SRI, GK, YD, YM
Analysis and interpretation of data; IMS, KS, EL, SS, PG, SD
Drafting of the manuscript: IMS, KS, EL, SS, PG, SD
Critical revision of the manuscript for important intellectual content: IMS, KS, EL, YM, RC, MGM, BSB, PSD, WJS, PG, SD
Statistical analysis: IMS, KS, SD
Obtained funding: PG, SD
Technical or material support: IMS, KS, EL, SS, MP, LPJ, SRI, YD, YM, MG, BSB, PSD
Study supervision: SD

*contributed equally
$Department of Medical Microbiology and Immunology, Faculty of Medicine, Assiut University, Egypt

Conflict of interest - Each author revealed that they do not have any competing financial and non-financial interests or connections, direct or indirect, or other situations that might raise the question of bias in the work reported or the conclusions, implications, or opinions stated here– including pertinent commercial or other sources of funding.

Once recruited, monocytes require ELMO1 to engulf the bacteria and propagate a robust TNF-α storm. These findings highlight that the dysregulated epithelial ELMO1→MCP-1 axis can serve as an early biomarker in the diagnostics of IBD and other inflammatory disorders.

Keywords

Intestinal inflammation; Inflammatory bowel disease; Microbial sensing and bacterial engulfment; epithelial-immune cell crosstalk; enteroid; monocyte-chemoattractant protein-1

INTRODUCTION

Intestinal microbes play an important role in cellular homeostasis. Single nucleotide polymorphisms (SNPs) of innate immune receptors, which are involved in bacterial recognition and clearance, are associated with the chronic intestinal inflammatory diseases [1-4]. For example, the variants of receptors such as NOD2 or TLRs that detect commensal and pathogenic bacteria are involved in the pathogenesis of Inflammatory Bowel Diseases (IBD) [5, 6]. IBD is associated with microbial dysbiosis, where a shift in the microbiota occurs toward more pro-inflammatory species. Microbial dysbiosis is characterized by the depletion of commensal bacteria from the members of the phyla *Firmicutes*, *Bacteroidetes*, and the enrichment of opportunistic pathogens from the phyla *Actinobacteria* and *Gamma proteobacteria* [7-9]. Adherent-invasive *E. coli* (*AIEC*) is the major pathovar of the species *Escherichia coli* that has been isolated from CD patients [10].

Our knowledge is limited about how the host signaling is influenced by microbial sensing linked to inflammatory diseases such as IBD. IBD is a multifactorial disease that affects 1.5 million people in the United States. [11, 12]. The treatment of IBD consists of corticosteroids, immunosuppressants, biologics, and in some cases, surgery, but no treatments are universally effective [13]. Thus, there is an urgent need to further understand the pathogenesis of IBD and the identification of new biomarkers in order to develop new therapeutics. One potential therapeutic approach is targeting the bacteria-mediated onset of inflammation. Generally, microbial dysbiosis and persistent infection could lead to the onset of chronic inflammation that is critical in IBD.

The recognition and internalization of a pathogen by a phagocytic receptor/mediator controls the downstream inflammatory responses [14, 15]. For example, after adhering and invading the gut epithelial cells, *AIECs* are engulfed by macrophages to induce inflammation [16]. The underlying mechanism by which pathogens breach host epithelium and generate inflammatory cytokine storm to initiate inflammatory diseases is unclear. We recently demonstrated that EnguLfment and cell MOtility protein 1 (ELMO1) is a microbial sensor that enables macrophages to engulf enteric bacteria, coordinately mount inflammation and orchestrates bacterial clearance [17-19]. ELMO1 binds to the Pattern Recognition Receptor (PRR) called Brain Angiogenesis Inhibitor-1 (BAI1), which recognizes bacterial Lipopolysaccharide (LPS) [20]. BAI1-ELMO1 signaling axis activates Rac1 and induces pro-inflammatory cytokines such as Tumor necrosis factor-α (TNF-α) and Monocyte Chemoattractant Protein 1 (MCP-1) [17, 21]. Genome-wide association studies (GWAS) have revealed the association of single nucleotide polymorphisms (SNPs) in ELMO1 with

IBD, rheumatoid arthritis (RA) kidney disease and diabetic nephropathy [22-24]. ELMO1 is required for the induction of several pro-inflammatory cytokines that are known to drive a plethora of inflammatory diseases, including IBD, cardiovascular diseases and RA [17]. Among them, MCP-1 is a chemokine, which plays a significant role in the recruitment of mononuclear cells to the site of inflammation; it is also one of the major cytokines involved in inflammatory diseases like IBD [25].

The function of ELMO1 in phagocytic cells was reported before [17, 26, 27]. However, its role in the non-phagocytic cells, i.e., the gut epithelium remains unknown. We hypothesized that the sensing of IBD-associated microbes by ELMO1 in the gut epithelium is the first line of host defense that may serve as an upstream trigger for immune cell-mediated cytokine storm. We used the cutting-edge stem cell-based- 3D enteroids as the model system to interrogate the role of ELMO1 in epithelial cells faced with the dysbiosis in IBD patients and defined a specific need the engulfment pathway to induce MCP-1. The generation of MCP-1 by the epithelium is followed by monocyte recruitment at the site of inflammation. Subsequently, bacteria enter the monocytes in an ELMO1-dependent manner and trigger the release of TNF-α, thereby, propagating the chronic inflammatory cascade that is the hallmark of IBD. In the DSS-mice model, the global, as well as myeloid-cell specific ELMO1−/− mice, had reduced colitis compared to WT mice. Our findings showed the possibility that targeting ELMO1 can simultaneously blunt both the ELMO1-MCP-1 and the ELMO1-TNF-α signaling axes in the epithelium and the macrophages, respectively, to combat the inflammation in IBD.

RESULTS

ELMO1 and MCP-1 are increased in IBD

In our previous study, we demonstrated that ELMO1 is involved in microbial sensing and controls intestinal inflammation [17]. To understand the role of ELMO1 in IBD, we analyzed publicly available datasets of 134 human subjects including healthy (60), CD (32) and UC (42) patients (Pubmed; Gene Expression Omnibus (GEO) datasets GSE83687 [28] and showed that ELMO1 and MCP-1 along with inflammatory cytokines were significantly increased in both CD and UC patients compared with healthy subjects (Table 1 and Fig. 1A). This finding was in parallel with human biopsy samples of IBD patients (Fig. 1B). The association between the levels of ELMO1 and MCP-1 was studied in the publicly available NCBI-GEO data-series where RNA Seq data from 214 normal colons showed that ELMO1 and MCP-1 genes display an equivalent Boolean relationship [29-31] in which, if the expression level of one gene is high, the other one is also high (Fig. 1C). These findings suggest a strong fundamental gene expression signature between the two genes that is conserved and invariant despite the population variance.

To determine if the elevated ELMO1 transcripts translate into elevated protein expression, we performed immunohistochemistry (IHC) on colonic biopsies from healthy controls and patients with UC or CD (Fig. 2A-D). ELMO1 expression was elevated both in the epithelium and in the lamina propria, but most strikingly in the diseased epithelium. We scored the level of ELMO1 staining in these colonic specimens, and ELMO1 was higher in IBD subjects compared to the healthy subjects (Fig. 2E).

Taken together, these findings indicate that expression of ELMO1 is elevated in colons of IBD patients. The expression was detected not only in the lamina propria but also in the epithelial lining, presumably contributed by infiltrating immune cells.

ELMO1 promotes DSS-induced colitis *in vivo*

To assess the effect of ELMO1 on the development of acute colitis, WT, and ELMO1$^{-/-}$ (global and myeloid cell-specific) mice were treated with 3.5% DSS added to the drinking water for 5 days. After 5 days, DSS was removed and the only freshwater was given to the mice for 4 days. DSS treatment induced a substantial weight loss at day 9 in WT mice compared to the ELMO1$^{-/-}$ mice (Fig. 3A, Supplementary Fig 1A) which was also reflected in the disease activity index (DAI, criteria as described in the method section) (Fig. 3B). In addition, the reduction in colon length, a marker of intestinal inflammation, was significantly less pronounced in DSS-treated ELMO1$^{-/-}$ mice (Fig. 3C-D). H&E staining demonstrated loss of crypts, dense infiltrates of leukocytes in both mucosa and submucosa, and thickening of the bowel wall only in DSS-treated WT mice. The pathology score was also significantly higher in WT mice colon tissue sections than ELMO1$^{-/-}$ colon tissue sections (Fig. 3E). Overall the degree of inflammation was significantly higher in WT mice than ELMO1$^{-/-}$ mice. During the DSS treatment, we recorded the death in WT mice (n=2) with all signs of inflammation, while we found unpredictable death in 1 ELMO1$^{-/-}$ mouse and no sign of inflammation in this mouse (Supplementary Fig. 1B).

ELMO1 is expressed both in epithelial cells and myeloid cells, including neutrophils and macrophages. To understand the effect of ELMO1 expressed on myeloid cells in DSS-mediated colitis, we assessed the role of ELMO1 in myeloid cell-specific (LysM-cre-driven) ELMO1-deficient mice. Similar to global KO mice, the degree of inflammation as shown by a reduction in the colon length was higher in LysM-cre negative WT mice compared to LysM-cre positive ELMO1 KO mice (Fig. 3C-D). Also, H&E staining demonstrated that the pathology score (demonstrated by loss of crypts, dense infiltrates of leukocytes in both mucosa and submucosa, and thickening of the bowel wall) was significantly higher in LysM cre negative WT mice than LysM cre positive ELMO1 KO mice (Fig 3E). Collectively these results indicate that the presence of ELMO1 increases the degree of colitis in DSS-treated mice as tested by global ELMO1$^{-/-}$ mice or myeloid cell-specific KO mice.

The gut-in-a-dish model to study the role of the host engulfment pathway

To investigate the role of ELMO1 in the IBD-afflicted gut epithelium, we used the stem-cell-derived 3D intestinal organoids or enteroids [32-35]. Enteroids mimic the *in vivo* condition, comprising four different cell types, namely epithelial, goblet, paneth and enterocytes [36-38]. Therefore, the use of intestinal crypt-derived enteroids nearly recreates the normal intestinal physiology. We generated both enteroids and enteroid-derived monolayers (EDMs, Fig. 4A, 4B) from colon specimens of the mouse or human biopsies obtained from healthy controls, UC and CD patients. The enteroids were polarized on transwells to generate the gut-in-a-dish model where the differentiated monolayers lost the expression of the stem-cell marker Lgr5 (Fig. 4B). To understand the role of epithelial ELMO1 following exposure to IBD-associated bacteria, we selected adherent-invasive *E. coli* (*AIEC*- LF82) as a model bacteria [10, 39, 40]. The advantage of the gut-in-a-dish model is that the EDMs can be

cocultured with the immune cells in the basal side (as we have done here with the monocytes) and bacteria in the apical side (as we have done here with the *AIEC*-LF82 on the top) (Fig. 4A). As shown in the schematic (Fig. 4A), the monolayer was collected for: a) invasion of bacteria by gentamicin protection assay, b) gene expression studies by qRT-PCR, c) staining of tight junction proteins, d) Supernatant from apical and basolateral side for ELISAs, e) monocyte recruitment assay with infected supernatant or with the infected monolayer as described later.

First, we confirmed that ELMO1 is indeed expressed in the human enteroids from colon and ileum by immunoblotting (Fig. 4C). Next, we assessed the level of ELMO1 in human enteroids by qRT-PCR (Fig. 5A) and western blot (Fig. 5B). The levels of ELMO1 transcripts and protein expression were elevated in UC and CD-derived enteroids compared to the healthy controls (Fig. 5A-B). The detailed description of the IBD subjects in Table 2 showed a broad range of patients and disease types in our cohort. As CD is a complex, heterogeneous disease, therefore it is possible that the CD enteroids from 8 different individuals showed variation in the expression of ELMO1. Interestingly, the increase of ELMO1 expression was positively tracked with the corresponding increase of the inflammatory markers MCP-1 in the CD subjects (Fig. 5A).

One of the major features of CD is the leaky barrier with the disruption of tight junction (TJ). Previously, it has been shown that *AIEC*-LF82 can disrupt polarized epithelia [41]. Here, we monitored the level of the TJ proteins (Zonula Occludin, ZO-1) in EDMs isolated from healthy and CD subjects (Fig. 5C). In healthy EDMs, disrupted TJs were seen only after infection with *AIEC*-LF82. In CD-derived EDMs, disrupted TJs were noted at the baseline and almost to a similar extent after infection with *AIEC*-LF82. Upon infection, the CD-derived EDMs showed increased levels of ZO1 at the TJs, which may be due to a short-term protective mechanism(s) that recruit ZO1 to resist infection/stress-induced TJ collapse.

ELMO1 is required for the engulfment of *AIEC*-LF82 within the gut epithelium.

Previously, we have shown that intestinal inflammation following engulfment of *Salmonella* was ELMO1 dependent [17]. To understand the role of ELMO1 in the internalization of the bacteria into epithelial cells, we used EDMs generated from colons of Wild type (WT) and ELMO1$^{-/-}$ mice. The depletion of ELMO1 in the EDMs from ELMO1$^{-/-}$ mice was confirmed by immunoblotting (Fig. 6A). Using the gentamicin protection assay [20, 42], we found that, the internalization of *AIEC-LF82* after 6 h of infection was decreased by 73% in ELMO1$^{-/-}$ EDMs compared to the WT EDMs (Fig. 6B).

EDM is a mixture of several cell types thus before pursuing functional studies, we tested if there is a difference in the cell types in murine-derived WT EDMs and ELMO1$^{-/-}$ EDMs. The specific markers of different cell types present in EDMs including carbonic anhydrase and sucrase-isomaltase for enterocyte markers, Muc-2 for goblet cell marker, lysozyme and β-defensin for Paneth cell marker, chromogranin A for enteroendocrine marker and DCLK-1 for tuft cell marker were examined. Fig. 6C showed that WT EDMs and ELMO1$^{-/-}$ EDMs do not have a significant difference in the cell types.

It has been reported that *E. coli* disrupts the epithelial tight junction (TJ) to enter the host tissue [43-45]. Therefore, confocal immunofluorescence studies were performed to monitor whether *AIEC-LF82* enters the epithelial cells through TJs. We found that in both WT and ELMO1$^{-/-}$ EDMs, the *AIEC*-LF82 entered through the epithelial TJs, as determined by ZO-1 staining that showed the bacteria were surrounded by ZO-1 (Fig. 6D). However, we found dissimilarities between both EDMs when it comes to the proximity of lysosomes to the invading pathogens. In WT EDMs, lysosomes (as detected using the lysosomal integral membrane protein, LAMP1) were found in close proximity to the invading *AIECs* (Fig. 6D), indicating that lysosomes were probably recruited to the site of TJ breach. Such observation was not seen in the ELMO1$^{-/-}$ EDMs. These findings raise the possibility that in the absence of lysosome targeting, ELMO1$^{-/-}$ EDMs may be defective not just in bacterial uptake, but also in bacterial clearance; as observed by ELMO1-mediated clearance of *Salmonella* [19]. It is not possible to perform the clearance assays in EDMs as the assay needs longer infection time when most of the infected EDMs will undergo extensive cell death within 8 – 12 h. To further confirm the function of ELMO1 in the clearance of enteric bacteria, we infected WT and ELMO1$^{-/-}$ mice with *Citrobacter rodentium*, a model bacteria that is cleared from host cells after 3–4 weeks of infection [46-48]. We counted the bacterial load in the fecal pellet of WT and ELMO1$^{-/-}$ mice feces at 4, 7, 14 and 21 days of post-infection. As expected on day 14 and 21 number of bacteria in fecal pellets of ELMO1$^{-/-}$ mice was remained significantly higher, relative to their WT counterparts (Supplementary Fig. 2A). Interestingly, at day 21, no bacteria were detected in the wild type mice. However, results were contrasting on day 4; this might be because of reduced bacterial uptake by ELMO1 (as observed in *Salmonella* before) (Supplementary Fig. 2A).

Taken together, these results showed that ELMO1 is required for *AIEC*-LF82 uptake through breaches in the epithelial TJs, and for the proper targeting of lysosomes to the invading *AIEC*-LF82 pathogen. Once internalized, ELMO1 may also be required for efficient clearance of the bacteria (studied in detail with macrophages later and Supplementary Fig. 2B).

ELMO1 in the gut epithelium is required for the generation of pro-inflammatory cytokine MCP-1 following infection with *AIEC*-LF82.

We previously showed that the ELMO1-mediated engulfment pathway is essential for the induction of pro-inflammatory cytokine such as MCP-1 from the monocytes [17]. Since the inflamed gut epithelium can express MCP-1 [49], which plays a major role in recruiting monocytes that in turn generates inflammatory cytokines in CD-afflicted gut [49-52], we hypothesized that ELMO1 may also be required for MCP-1 production by the gut epithelium once it is breached by invading *AIEC*-LF82.

To determine that the production of MCP-1 from the epithelium is ELMO1 dependable, we measured the levels of MCP-1 transcript by qRT-PCR (Fig. 7A) and by ELISA (Fig. 7B) in WT and ELMO1$^{-/-}$ EDMs either uninfected or infected with *AIEC*-LF82. In WT EDMs, MCP-1 was undetectable without infection, but its levels were elevated after infection. Interestingly, the induction of MCP-1 following infection was blunted in ELMO1$^{-/-}$ EDMs

(Fig 7A-B) indicating that ELMO1 is required for the generation of MCP-1 by the epithelium after infection with IBD-associated bacteria.

An intact ELMO1/MCP-1 axis in the gut epithelium is required for the recruitment of monocytes to the infected epithelium

CCL2/MCP-1$^{-/-}$ mice had a significant reduction in monocyte recruitment in inflammatory models in the secondary pulmonary granulomata in response to *Schistosoma mansoni* eggs [53, 54]. To investigate the role of the ELMO1/ MCP-1 axis in the recruitment of monocytes, we infected the WT and ELMO1$^{-/-}$ EDMs with *AIEC*-LF82 for 6 h and assessed the ability of these EDMs to recruit monocytes. After the infection, either the infected monolayer itself (Fig. 7C) or the conditioned supernatant (Fig. 7D) was co-cultured with monocytes, and the monocytes toward the infected EDM site were assessed. Our result showed that the monocyte recruitment toward *AIEC*-LF82-infected ELMO1$^{-/-}$ EDMs and towards its supernatant were significantly lower compared to the WT EDMs (Fig 7E, Fig. Supplement 3). Further, we compared the monocyte migration toward the supernatant derived from *AIEC*-LF82-infected WT EDMs and *AIEC*-LF82-infected ELMO1$^{-/-}$ EDMs. ELMO1$^{-/-}$ EDMs displayed a 50% reduction in monocyte recruitment (Fig 7E-F). These results indicate that ELMO1-dependent MCP-1 production by the gut epithelium could serve as an upstream cue for monocyte recruitment to the sites of infection. To confirm our conclusion, we used two antibodies that could neutralize MCP-1. In the presence of neutralizing antibodies, monocyte recruitment toward the infected supernatants collected from WT and ELMO1$^{-/-}$ EDMs was hampered (Fig 7G). As infection can induce cell death, we monitored the amount of cell death by the LDH assay using supernatants collected from Fig. 6 A-B and E. The WT and ELMO1$^{-/-}$ EDMs showed no remarkable cell death in the untreated conditions. Following infection, cell death was increased that was higher in WT compared to the ELMO1$^{-/-}$ EDMs (Fig. 7H).

ELMO1 in macrophages is essential for the engulfment of *AIEC*-LF82, and the generation of pro-inflammatory cytokines

As macrophages are recruited to the sites of *AIEC*-LF82 infection, we determined the role of ELMO1 in the internalization of *AIEC*-LF82 in macrophages. We used the gentamicin protection assay to assess bacterial uptake in ELMO1-depleted J774 macrophages[17]. The expression of ELMO1 was evaluated in control and ELMO1 shRNA cells (Fig. 8A*),* where around 90% depletion of ELMO1 was confirmed by immunoblotting. In the gentamicin protection assay, ELMO1-depleted cells showed an approximately 50% reduction in bacterial internalization compared to WT cells (Fig. 8B).

To determine whether ELMO1 is essential for the clearance of *AIEC*-LF82 (as observed in *Salmonella* [19]), bacterial engulfment and clearance were studied at 30 min, 3, 6, 12 and 24 h in the murine macrophage cell line J774 (Supplementary Fig. 2B). ELMO1$^{-/-}$ cells showed lower uptake of *AIEC*-LF82 compared to WT macrophages (50% reduction) at 30 min, but retention of a higher bacterial load at later time points (3 fold increase at 24 h after infection). These findings indicate that ELMO1 is required not only for uptake but also for the clearance of *AIEC*-LF82.

To assess the contribution of ELMO1 in bacterial internalization in a more physiologically relevant system, we carried out the gentamicin protection assay using primary intestinal macrophages isolated from WT or ELMO1$^{-/-}$ mice (Fig. 8C). While intestinal macrophages from WT mice engulfed bacteria efficiently, bacterial uptake was 60% decreased in macrophages from ELMO1$^{-/-}$ mice, indicating that ELMO1 is essential for the engulfment of *AIEC*-LF82 in macrophages.

TNF-α is the major pro-inflammatory cytokine that is elevated early in the development of CD [49, 55]. Macrophages exposed to *AIECs* engulf the bacteria and can induce TNF-α [49]. Here we show that lack of ELMO1 in J774 macrophage decreased the TNF-α protein secretion when infected with *AIEC*-LF82 (Fig. 8D). These findings are consistent with our previous findings with *Salmonella* [17] that ELMO1 is essential for TNF-α production from the macrophage upon bacterial engulfment.

Discussion

In most chronic diseases, including inflammatory bowel disease (IBD), a significant proportion of the patients do not respond to the current medications. Therefore, there is an urgent need to identify biomarkers in the earlier stages of the disease. Inflammation is a common factor in all these diseases and microbial sensing in the intestinal tract is critical to initiate the inflammation. Here, we identified the role of ELMO1 (Engulfment and Cell Motility Protein-1) as a microbial sensor that turns on the inflammatory signals in IBD. Previously, we have shown that ELMO1 is involved in murine intestinal inflammation following enteric infection and engulfment of bacteria in phagocytes. Using a stem-cell-based “gut-in-a-dish” coculture model, we identified the role of ELMO1 in epithelial and as well as in phagocytic cells. The model was developed to study the interactions between microbes, epithelium, and monocytes in the context of inflammatory bowel disease (IBD). We found the host ELMO1 facilitates the engulfment of pathogenic IBD-associated bacteria (*AIEC*-LF82) in the gut epithelium, triggers the induction of the pro-inflammatory cytokine, MCP-1; which later helps in monocytes recruitment from peripheral blood to the site of local inflammation (Fig. 7E-G). Next, we showed that the same molecule, ELMO1 is also essential for the uptake and clearance of *AIEC*-LF82 in the macrophages, and is required for coordinately mounting yet another pro-inflammatory cytokine response, TNF-α. This ELMO1-TNF-α axis presumably feeds forward to propagate inflammation in the gut by triggering the activation of other immune cells like monocytes and T cells. Thus, the two signaling axes, ELMO1/MCP-1 and ELMO1/TNF-α, orchestrated by the same engulfment pathway in two different cell types, the epithelium and the macrophage, respectively, appear to be working as ‘first’ and ‘second’ responders respectively to combat pathogenic microbes, thereby relaying distress signals from one cell type to another as the microbe invades through the breached mucosal barrier (Fig 8E).

This work also provides the first mechanistic insights into how luminal dysbiosis initiates inflammation in the gut. Bacterial clearance and microbial dysbiosis are one of the hallmarks of IBD that control the outcome of innate immune responses. Healthy commensals like *Bacteroidetes* and *Faecalibacterium prausnitzii* are decreased in patients with CD, while pathogenic microbes like invasive *Escherichia coli, Serratia marcescens*,

Cronobacter sakazakii and *Ruminoccus gnavus* are increased [8, 9, 16, 56]. A dysbiotic microbial population can harbor pathogen and pathobionts that can aggravate intestinal inflammation or manifest systemic disease. Effector proteins produced by pathogenic bacteria can activate signaling that induces granuloma formation; one of the key symbols in CD pathogenesis [57]. In CD granuloma, the number of mucosal adherent invasive *E. coli* is higher because of defective clearance that can cause dysbiosis [7, 58]. Previously we showed that ELMO1 and the engulfment-pathway in the professional phagocytes are essential for the internalization of *Salmonella,* and for mounting intestinal inflammation [17]. In this work, we have demonstrated the role of ELMO1 in non-phagocytic epithelial cells using the gut-in-a-dish model, in the context of IBD using the IBD-associated microbe *AIEC-LF82*. In the DSS-treated ELMO1$^{-/-}$ mice (either global or the myeloid-cell driven) has less pronounced colitis. Previous work from Zheng *et al*., showed that ELMO1 is overexpressed in inflamed colonic tissue than the corresponding non-inflamed tissues of 18 IBD patients and ELMO1 overexpression increased wound healing in Rac 1-dependent manner. Also, they demonstrated that the overexpression of ELMO1 by tail vein injection of pSin-EF2-ELMO1-Pur plasmid attenuated colonic inflammation and promoted recovery after DSS-mediated colonic injury [59]. Contrary to Zheng et al., we showed that ELMO1$^{-/-}$ KO mice developed less colitis than WT mice after DSS treatment. The discrepancy between the two studies probably because of the two different approaches: overexpression by a plasmid in Zheng et al. and KO mice model in the current study. The result could be attributed to the level of ELMO1 in the colon which can determine the degree of colitis. In our study, we have used WT and ELMO1$^{-/-}$ KO mice where ELMO1 is completely diminished in global KO mice or diminished only in myeloid cells in LysM Cre mice, therefore we could assess the essential role of ELMO1 in the colonic inflammation. While the study of Zheng et al. showed that overexpression of ELMO1 could attenuate the colitis after DSS treatment, but the baseline level of ELMO1 was not mentioned in the study, therefore it is not known the level of ELMO1 that could be associated with either inflammation or recovery. Importantly, our result agreed to Zheng et al., in the association of ELMO1 with inflammation in IBD subjects. They showed that ELMO1 is overexpressed in inflamed colonic tissues than the corresponding non-inflamed tissue in 18 IBD patients. Interestingly, ELMO1 interacting partner BAI1 also showed protection after DSS-treatment [60]. It suggests that ELMO1 may act as a gatekeeper in the BAI1/ELMO1-mediated signaling that senses bacteria and maintains the balance of inflammation.

The effect of ELMO1 in bacterial clearance was also observed in *Citrobacter*-infected WT and ELMO1$^{-/-}$ specimens. The use of colonic enteroids from ELMO1$^{-/-}$ mice, either alone or in co-cultures with monocytes allowed us to interrogate the function of ELMO1 in the epithelium and in the monocytes separately. It is not possible to perform the *in vivo* model of *AIEC*-LF82 infection using our ELMO1$^{-/-}$ mice as the strain cannot colonize or provide gut inflammation unless the mice are modified as transgenic CEABAC10 mouse model expressing human CEACAMs [61]. Therefore, the complete impact of ELMO1 in chronic inflammatory diseases needs further investigation.

By showing that the ELMO1/MCP-1 axis is an early step in gut inflammation, this work provides rationale and impetus for the development of anti-MCP-1 biologics to treat IBD. MCP-1 belongs to a CC chemokine subfamily, and its effects are mediated through CC

chemokine receptor 2 (CCR2). So far, in human, only A2518G variation in the MCP-1 gene promoter has been associated with CD [62]. However, MCP-1 is not just important in IBD but also involved in other inflammatory diseases, such as atherosclerosis [63]. MCP-1 promotes the balance between anti-inflammatory and pro-inflammatory responses to infection. Treatment with recombinant MCP-1/CCL2 increases bacterial clearance and protects mice that are systemically infected with *Pseudomonas aeruginosa* or *Salmonella typhimurium* [64]. Administration of MCP-1 can increase chemotaxis of murine macrophages, enhance phagocytosis and killing of bacteria [64], whereas pretreatment of mice with anti-MCP-1/CCL2 impaired bacterial clearance. Therefore, increased expression of MCP-1 by ELMO1 in intestinal epithelium after exposure to *AIEC*-LF82 is likely to have two-fold importance-- 1) for controlling the increased bacterial load by killing the bacteria, and 2) for promoting monocyte recruitment and activation, which initiate a pro-inflammatory cytokine storm by inducing TNF-α from macrophages. Further work is required before we can begin to assess the safety and efficacy of anti-MCP-1 therapies in IBD.

Until now, the majority of IBD-related research and therapeutic strategies have remained focused on T cell responses and on neutralizing the impact of TNF-α. Our work provides mechanistic insights into some of the upstream/initial immune responses that play out in the epithelium and within the macrophages upon sensing luminal dysbiosis. We defined an upstream event that could be exploited to develop biomarkers, and eventually interrogated for the identification of strategies for therapeutic intervention (e.g., anti-MCP-1 therapy, as discussed later). The need for an in-depth understanding of nature and the extent of the contribution of epithelial cells and/or monocytes in disease progression is urgent because of the limited efficacy of the available treatment regimens [65]. Because the recruitment of monocytes from circulation to the site of infection/inflammation is a key early event in inflammatory diseases of the gut, the ELMO1→MCP-1 axis we defined here, is potentially an actionable high value diagnostic and therapeutic target in IBD. Detection of high levels of ELMO1 in the epithelium could serve as an early indicator of activation of the engulfment pathway, and hence, could serve as a surrogate diagnostic marker of early inflammation due to luminal dysbiosis. Similarly, targeting the engulfment pathway is expected to restore immune homeostasis and resolve chronic inflammation via a completely novel approach that could synergize with existing therapies, and thereby, improve response rates and rates of sustained remission.

MATERIALS AND METHODS

All methods involving human and animal subjects were performed in accordance with the relevant guidelines and regulations of the University of California San Diego and the NIH research guidelines.

Human Subjects

All the IBD patients' were seen at the University of California, San Diego at the IBD-Center. They were recruited and consented using a study proposal approved by the Institutional Review Board of the University of California, San Diego. For immunohistochemical

analysis of human tissue specimens, human colonic biopsies from healthy controls and patients with active UC or CD were retrospectively obtained from routine colonoscopies and provided by the section of Gastroenterology, VA San Diego Healthcare System, following the protocol approved by the Human Research Protection Program (hrpp) Institutional Review Board (IRB). All the tissues for RNA isolation and for the isolation of enteroids were collected from healthy and IBD subjects' enrolled in the IBD-Center of the University of California, San Diego following the approved research protocol of hrpp IRB. Each human participants were aware and signed the consent form approved by the hrpp IRB, to agree that the colonic specimens from their colonoscopy will be used as a tissue source or to generate an enteroid line for functional studies. The clinical phenotype and information were assessed by an IBD specialist.

Animals

WT and ELMO1$^{-/-}$, C57BL/6 mice were gender- and age-matched littermate that was used to isolate intestinal crypts and macrophages. WT and ELMO1$^{-/-}$ KO mice were infected orally with *Citrobacter rodentium* (5×10^8 cfu) and the fecal pellet was collected at different time points (4, 7, 14 and 21 days) to measure the bacterial load. Animals were bred, housed, used for all the experiments and euthanized according to the University of California San Diego Institutional Animal Care and Use Committee (IACUC) policies under the animal protocol number S18086. *All methods were carried out in accordance with relevant guidelines and regulations and the experimental protocols were approved by institutional policies and reviewed by the licensing committee.*

Bacteria and bacterial culture

Adherent Invasive *Escherichia coli* strain LF82 (*AIEC*-LF82), isolated from the specimens of Crohn's disease patient, was obtained from Arlette Darfeuille-Michaud [10]. A single colony was inoculated into LB broth and grown for 8 h under aerobic conditions and then under oxygen-limiting conditions. Cells were infected with a multiplicity of infection (moi) of 10.

Cell lines and cell culture

Control and ELMO1 small-hairpin RNA (shRNA) macrophage (J774) cells were maintained in high glucose Dulbecco's modified Eagle's medium (DMEM) containing 10% fetal calf serum, as described previously[17]. THP-1 cells were maintained in RPMI media containing 10 mM HEPES, 10 % FBS at a cell concentration of lower than 10^6 cells/ml [21].

Isolation of enteroids from colonic specimens of mouse and human

Intestinal crypts were isolated from the colonic tissue specimen by digesting with Collagenase type I [2 mg/ml; Invitrogen] and cultured in stem-cell enriched conditioned media with WNT 3a, R-spondin and Noggin [33, 34, 66]. Briefly, the crypts after digestion with Collagenase were filtered with a cell strainer and washed with medium (DMEM/F12 with HEPES, 10% FBS), After adding collagenase I solution containing gentamicin (50 μg/ml, Life Technologies) and mixing thoroughly, the plate was incubated at 37° C inside a CO_2 incubator for 10 min, with vigorous pipetting between incubations and monitoring the

intestinal crypts dislodging from tissue. The collagenase was inactivated with media and filtered using a 70-μm cell strainer over a 50-ml centrifuge tube. Filtered tissue was spun down at 200 g for 5 min and the media was aspirated. The epithelial units were suspended in matrigel (BD basement membrane matrix). The cell-matrigel suspension (15 μl) was placed at the center of the 24-well plate on ice and placed on the incubator upside-down for polymerization. After 10 min, 500 μl of 50% conditioned media (prepared from L-WRN cells with Wnt3a, R-spondin and Noggin, ATCC® CRL-3276™ [33]) containing 10 μM Y27632 (ROCK inhibitor) and 10 μM SB431542 (an inhibitor for TGF-β type I receptor) were added to the suspension. For the human colonic specimens, a proprietary cocktail was added to the above media. The medium was changed every 2 days and the enteroids were expanded and frozen in liquid nitrogen.

The preparation of Enteroid-derived monolayers (EDMs)

To prepare EDMs, single cells from enteroids in 5% conditioned media was added to diluted Matrigel (1:30) as done before [67]. In some cases, the EDMs were also differentiated for 2 days in advanced DMEM/F12 media without Wnt3a but with R-spondin, Noggin, B27 and N2 supplements and 10 μM ROCK inhibitor [34]. As expected, this results in a marked reduction in the expression of the stemness marker lgr5 in EDMs [34].

For all functional assays, experiments were performed multiple times with EDMs-derived from enteroids collected from at least 3 different mice, including both the genders.

Isolation of murine intestinal macrophages

Murine intestinal macrophages were isolated using methods described previously [17, 19, 20]. Briefly, small intestines were collected and intestinal fragments were digested with enzyme cocktail including collagenase (Miltenyi Biotec). The cell suspension was passed through a cell strainer to remove debris, and enriched with $CD11b^+$ cells using the CD11b MACS kit (Miltenyi Biotec). Intestinal macrophages were labeled using monoclonal antibody CD11b (BD Biosciences) and sorted using a FACS Vantage (BD Biosciences). The purity of intestinal macrophages was determined by staining with an antibody specific for the macrophage marker F4/80.

Bacterial internalization by gentamicin protection assay

Approximately 2×10^5 cells were plated onto a 0.4 μm pore transwell insert and infected with bacteria with moi 10. Bacterial internalization was determined after 6 h of infection of WT and $ELMO1^{-/-}$ EDMs with *AIEC*-LF82 by gentamicin protection assay [17, 20].

Monocyte Recruitment Assay to Determine the Function of ELMO1 and MCP-1

WT and ELMO1−/− EDMs were plated in the transwell for polarization and infected with *AIEC*-LF82 for 6 h. Supernatant from the basolateral chamber was collected and placed in the new 24-well plate, and 6.5 mm 8-μm pore-sized transwells (Costar) where THP-1 cells or peripheral blood-derived monocytes in OptiMEM (Gibco) were placed on the apical chamber. In another assay, the EDM layer was collected and flipped and placed on the bottom of the transwell.

The number of recruited live monocytes was measured after 1, 2, 8, 16 and 24 h. We compared the number of recruited monocytes toward supernatants collected from uninfected and *AIEC*-LF82 infected cells in WT and ELMO1$^{-/-}$ EDMs. To understand the role of MCP-1, supernatants were collected from *AIEC*-LF82 infected EDMs, followed by incubation with anti-MCP-1 antibodies, either 2H5 Ab (monoclonal antibody from eBioscience with a dilution of 1:100) or NBP1 Ab (Novus Biologicals with a dilution of 1:200) for 2 h. The coculture of EDMs with monocytes was performed using monocytes (2×10^6 cells of THP-1) added to the apical part of 6.5 mm 8-μm pore-sized transwells. The number of living recruited monocytes were counted after 16 h.

Cytokine Assays

Supernatants were collected from the basolateral chamber of the uninfected and *AIEC*-LF82 infected cells. MCP-1 was measured using the Mouse CCL2 (MCP-1) ELISA Ready-Set-Go Kit according to the manufacturer's instructions (eBioscience). Supernatants were collected from control or ELMO1-depleted J774 cells after *AIEC*-LF82 infection and TNF-α was measured using the ELISA kit from BD bioscience.

RNA Preparation, Real-Time Reverse-Transcription Polymerase Chain Reaction

After infection with *AIEC*-LF82 EDMs were collected for RNA isolation followed by quantitative RT-PCR as described in detail in the Supplementary Materials and Methods.

Immunohistochemistry and the scoring of ELMO1 expression

The colonic specimens of known histologic type (8 normal colorectal tissue; 5 ulcerative colitis and 5 Crohn's disease) were analyzed by IHC using the anti-ELMO1 antibody (1:40, an anti-rabbit antibody from Novus). Briefly, formalin-fixed, paraffin-embedded tissue sections of 4 μm thickness were cut and placed on glass slides coated with poly-L-lysine, followed by deparaffinization and hydration. Heat-induced epitope retrieval was performed using citrate buffer (pH-6) in a pressure cooker. Tissue sections were incubated with 0.3% hydrogen peroxidase for 15 min to block endogenous peroxidase activity, followed by incubation with primary antibodies for 30 min in a humidified chamber at Room temperature. Immunostaining was visualized with a labeled streptavidin-biotin using 3, 3′-diaminobenzidine as a chromogen and counterstained with hematoxylin. For the scoring of ELMO1, all the samples were first quantitatively analyzed and scored based on the intensity of staining was scored on a scale of 0 to 3, where 0 = no staining, 1 = light brown, 2 = brown, and 3 = dark brown.

Gene expression analysis

The association between the levels of ELMO1 and MCP-1 (*CCL2*) mRNA expression was tested in a cohort of normal colon tissue as described in details in the Supplementary Materials and Methods. Briefly, the mRNA expression level of ELMO1 was detected in healthy, CD and UC populations, using publicly available NCBI-GEO data-series (GSE83687) where the cohort has 60 healthy, 42 CD, and 32 UC subjects. The detailed information of the cohort with other inflammatory cytokines are included in Table 1.

Induction of Colitis in Murine Model

The ELMO1$^{-/-}$ mice (global and Myeloid-cell specific) and WT mice (8–10 weeks, gender-matched) were given either normal drinking water (control) or 3.5% dextran sodium sulfate (DSS) dissolved in the drinking water for 5 d, followed by an additional 4 d recovery period with normal drinking water. Equal water volumes were added to all mice groups and the amount of water consumed was measured at the end of treatment. Weight of the mice was measured before DSS treatment, then monitored daily and the percentage of weight loss was determined. Disease activity index (DAI) was calculated using by scoring stool consistency (0–4), rectal bleeding (0–4), and weight loss (0–4) as previously published [68]. Mice were sacrificed, colon length was measured, and colon samples were collected for assessing histology score [69] by using H&E staining.

LDH Assay

Enteriod-derived monolayer (EDM) of WT and ELMO$^{-/-}$ cell at a density of 2× 10^5 cell/well were seeded in trans well as described previously. The EDMs were challenged or not with LF82 at moi 10. Supernatants were collected from uninfected and infected EDMs and assayed for LDH assay using LDH-Glo™ Cytotoxicity Assay kit (Promega) according to the manufacturer's instruction. Briefly, supernatants were diluted 1/100 in LDH storage buffer, then an equal volume of LDH Detection Reagent was added to the diluted sample (1:1). The mixture was incubated for 60 minutes at room temperature and the LDH activity was determined by measurement of luminescence. To assess the assay performance and linearity, an LDH positive control (purified Lactate Dehydrogenase from rabbit muscle) was included in each assay. Serial dilutions from the LDH positive control (32–0.5 mU/ml) was done and included in our experiments. Culture media was used to determine the medium background.

Confocal Microscopy

WT and ELMO1$^{-/-}$ EDMs were plated onto 8-well chamber slides (Millicell) and infected with bacteria with moi 10. After infection, cells were stained for LAMP-1 (Lysosomal Associated Membrane Protein-1) and ZO1 (Zonula Occludens) following the protocols as mentioned in the Supplementary Materials and Methods.

Statistical analysis

Bacterial internalization, monocyte recruitment assays and ELISA results were expressed as the mean ± SD / SEM and compared using a two-tailed Student's t-test. Results were analyzed in the Graph pad Prism and considered significant if p values were < 0.05.

Supplementary Material

Refer to Web version on PubMed Central for supplementary material.

Acknowledgment

This work was supported by NIH grants DK107585, DK099275; NIH CTSA grant UL1TR001442 (to S.D), CA100768, CA160911 and DK099226 (to P.G). A part of the work with human subjects with Crohn's disease was supported by Leonna M Helmsley Charitable Trust (to S.D and P.G). S.R.I was supported by NIH Diversity Supplement award (3R01DK107585-02S1) and Y.M was supported by NIH Training Grant in Gastroenterology (T32DK0070202). We appreciate the contribution of Dr. Debashis Sahoo, Department of Pediatrics for providing

the access to the Boolean analysis and the Hegemon software. We are thankful to Mitchel Lau and Julian Tam for technical support; Lee Swanson for discussing the DSS-mediated colitis and to Drs. Ernst, Crowe, Barrett and Eckmann for providing the access to the shared equipment within the UCSD GI division. We are grateful to Rama Pranadinata (Project Manager of HUMANOID CoRE); Mackenzie Fuller, Dominik Stec and Courtney Tindle (employees of HUMANOID CoRE) for isolation, culture and biobanking of healthy, CD and UC-derived enteroids.

Abbreviations:

IBD	Inflammatory Bowel Disease
UC	Ulcerative Colitis
CD	Crohn’s Disease
AIEC	Adherent-Invasive *E. coli*
TNF-α	Tumor Necrosis Factor -α
MCP-1	Monocyte chemoattractant protein-1
EDM	Enteroid-derived monolayer
ELMO1	Engulfment and cell motility protein 1
LPS	Lipopolysaccharide

References

1. Moustafa A, Li W, Anderson EL, Wong EHM, Dulai PS, Sandborn WJ, Biggs W, Yooseph S, Jones MB, Venter JC, Nelson KE, Chang JT, Telenti A & Boland BS (2018) Genetic risk, dysbiosis, and treatment stratification using host genome and gut microbiome in inflammatory bowel disease, Clin Transl Gastroenterol. 9, e132. [PubMed: 29345635]
2. Manichanh C, Borruel N, Casellas F & Guarner F (2012) The gut microbiota in IBD, Nat Rev Gastroenterol Hepatol. 9, 599–608. [PubMed: 22907164]
3. Miyoshi J & Chang EB (2017) The gut microbiota and inflammatory bowel diseases, Transl Res. 179, 38–48. [PubMed: 27371886]
4. Ni J, Wu GD, Albenberg L & Tomov VT (2017) Gut microbiota and IBD: causation or correlation?, Nat Rev Gastroenterol Hepatol. 14, 573–584. [PubMed: 28743984]
5. Hugot JP, Chamaillard M, Zouali H, Lesage S, Cezard JP, Belaiche J, Almer S, Tysk C, O'Morain CA, Gassull M, Binder V, Finkel Y, Cortot A, Modigliani R, Laurent-Puig P, Gower-Rousseau C, Macry J, Colombel JF, Sahbatou M & Thomas G (2001) Association of NOD2 leucine-rich repeat variants with susceptibility to Crohn's disease, Nature. 411, 599–603. [PubMed: 11385576]
6. Ogura Y, Bonen DK, Inohara N, Nicolae DL, Chen FF, Ramos R, Britton H, Moran T, Karaliuskas R, Duerr RH, Achkar JP, Brant SR, Bayless TM, Kirschner BS, Hanauer SB, Nunez G & Cho JH (2001) A frameshift mutation in NOD2 associated with susceptibility to Crohn's disease, Nature. 411, 603–6. [PubMed: 11385577]
7. Frank DN, St Amand AL, Feldman RA, Boedeker EC, Harpaz N & Pace NR (2007) Molecular-phylogenetic characterization of microbial community imbalances in human inflammatory bowel diseases, Proc Natl Acad Sci U S A. 104, 13780–5. [PubMed: 17699621]
8. Forbes JD, Van Domselaar G & Bernstein CN (2016) The Gut Microbiota in Immune-Mediated Inflammatory Diseases, Front Microbiol. 7, 1081. [PubMed: 27462309]
9. Oberc A & Coombes BK (2015) Convergence of External Crohn's Disease Risk Factors on Intestinal Bacteria, Front Immunol. 6, 558. [PubMed: 26579131]
10. Darfeuille-Michaud A, Boudeau J, Bulois P, Neut C, Glasser AL, Barnich N, Bringer MA, Swidsinski A, Beaugerie L & Colombel JF (2004) High prevalence of adherent-invasive

Escherichia coli associated with ileal mucosa in Crohn's disease, Gastroenterology. 127, 412–21. [PubMed: 15300573]

11. Baumgart DC & Sandborn WJ (2012) Crohn's disease, Lancet. 380, 1590–605. [PubMed: 22914295]
12. Kugathasan S, Judd RH, Hoffmann RG, Heikenen J, Telega G, Khan F, Weisdorf-Schindele S, San Pablo W Jr., Perrault J, Park R, Yaffe M, Brown C, Rivera-Bennett MT, Halabi I, Martinez A, Blank E, Werlin SL, Rudolph CD, Binion DG & Wisconsin Pediatric Inflammatory Bowel Disease, A. (2003) Epidemiologic and clinical characteristics of children with newly diagnosed inflammatory bowel disease in Wisconsin: a statewide population-based study, J Pediatr. 143, 525–31. [PubMed: 14571234]
13. Baran B & Karaca C (2013) Practical medical management of Crohn's disease, ISRN Gastroenterol. 2013, 208073. [PubMed: 24307950]
14. Ishii KJ, Koyama S, Nakagawa A, Coban C & Akira S (2008) Host innate immune receptors and beyond: making sense of microbial infections, Cell Host Microbe. 3, 352–63. [PubMed: 18541212]
15. Barton GM (2008) A calculated response: control of inflammation by the innate immune system, J Clin Invest. 118, 413–20. [PubMed: 18246191]
16. Chassaing B & Darfeuille-Michaud A (2011) The commensal microbiota and enteropathogens in the pathogenesis of inflammatory bowel diseases, Gastroenterology. 140, 1720–28. [PubMed: 21530738]
17. Das S, Sarkar A, Choudhury SS, Owen KA, Castillo V, Fox S, Eckmann L, Elliott MR, Casanova JE & Ernst PB (2015) ELMO1 has an essential role in the internalization of Typhimurium into enteric macrophages that impacts disease outcome, Cell Mol Gastroenterol Hepatol. 1, 311–324. [PubMed: 26878033]
18. McCormick BA (2015) ELMO1: More Than Just a Director of Phagocytosis, Cell Mol Gastroenterol Hepatol. 1, 262–263. [PubMed: 28210678]
19. Sarkar A, Tindle C, Pranadinata RF, Reed S, Eckmann L, Stappenbeck TS, Ernst PB & Das S (2017) ELMO1 Regulates Autophagy Induction and Bacterial Clearance During Enteric Infection, J Infect Dis. 216, 1655–1666. [PubMed: 29029244]
20. Das S, Owen KA, Ly KT, Park D, Black SG, Wilson JM, Sifri CD, Ravichandran KS, Ernst PB & Casanova JE (2011) Brain angiogenesis inhibitor 1 (BAI1) is a pattern recognition receptor that mediates macrophage binding and engulfment of Gram-negative bacteria, Proceedings of the National Academy of Sciences of the United States of America. 108, 2136–41. [PubMed: 21245295]
21. Das S, Sarkar A, Ryan KA, Fox S, Berger AH, Juncadella IJ, Bimczok D, Smythies LE, Harris PR, Ravichandran KS, Crowe SE, Smith PD & Ernst PB (2014) Brain angiogenesis inhibitor 1 is expressed by gastric phagocytes during infection with Helicobacter pylori and mediates the recognition and engulfment of human apoptotic gastric epithelial cells, FASEB J. 28, 2214–24. [PubMed: 24509909]
22. Parmar AS, Lappalainen M, Paavola-Sakki P, Halme L, Farkkila M, Turunen U, Kontula K, Aromaa A, Salomaa V, Peltonen L, Halfvarson J, Torkvist L, D'Amato M, Saavalainen P & Einarsdottir E (2012) Association of celiac disease genes with inflammatory bowel disease in Finnish and Swedish patients, Genes Immun. 13, 474–80. [PubMed: 22592522]
23. Pezzolesi MG, Katavetin P, Kure M, Poznik GD, Skupien J, Mychaleckyj JC, Rich SS, Warram JH & Krolewski AS (2009) Confirmation of genetic associations at ELMO1 in the GoKinD collection supports its role as a susceptibility gene in diabetic nephropathy, Diabetes. 58, 2698–702. [PubMed: 19651817]
24. Whitaker JW, Boyle DL, Bartok B, Ball ST, Gay S, Wang W & Firestein GS (2015) Integrative omics analysis of rheumatoid arthritis identifies non-obvious therapeutic targets, PLoS One. 10, e0124254. [PubMed: 25901943]
25. Singh UP, Singh NP, Murphy EA, Price RL, Fayad R, Nagarkatti M & Nagarkatti PS (2016) Chemokine and cytokine levels in inflammatory bowel disease patients, Cytokine. 77, 44–9. [PubMed: 26520877]

26. deBakker CD, Haney LB, Kinchen JM, Grimsley C, Lu M, Klingele D, Hsu PK, Chou BK, Cheng LC, Blangy A, Sondek J, Hengartner MO, Wu YC & Ravichandran KS (2004) Phagocytosis of apoptotic cells is regulated by a UNC-73/TRIO-MIG-2/RhoG signaling module and armadillo repeats of CED-12/ELMO, Curr Biol. 14, 2208–16. [PubMed: 15620647]
27. Gumienny TL, Brugnera E, Tosello-Trampont AC, Kinchen JM, Haney LB, Nishiwaki K, Walk SF, Nemergut ME, Macara IG, Francis R, Schedl T, Qin Y, Van Aelst L, Hengartner MO & Ravichandran KS (2001) CED-12/ELMO, a novel member of the CrkII/Dock180/Rac pathway, is required for phagocytosis and cell migration, Cell. 107, 27–41. [PubMed: 11595183]
28. Peters LA, Perrigoue J, Mortha A, Iuga A, Song WM, Neiman EM, Llewellyn SR, Di Narzo A, Kidd BA, Telesco SE, Zhao Y, Stojmirovic A, Sendecki J, Shameer K, Miotto R, Losic B, Shah H, Lee E, Wang M, Faith JJ, Kasarskis A, Brodmerkel C, Curran M, Das A, Friedman JR, Fukui Y, Humphrey MB, Iritani BM, Sibinga N, Tarrant TK, Argmann C, Hao K, Roussos P, Zhu J, Zhang B, Dobrin R, Mayer LF & Schadt EE (2017) A functional genomics predictive network model identifies regulators of inflammatory bowel disease, Nat Genet. 49, 1437–1449. [PubMed: 28892060]
29. Sahoo D (2012) The power of boolean implication networks, Front Physiol. 3, 276. [PubMed: 22934030]
30. Sahoo D, Dill DL, Gentles AJ, Tibshirani R & Plevritis SK (2008) Boolean implication networks derived from large scale, whole genome microarray datasets, Genome Biol. 9, R157. [PubMed: 18973690]
31. Sahoo D, Seita J, Bhattacharya D, Inlay MA, Weissman IL, Plevritis SK & Dill DL (2010) MiDReG: a method of mining developmentally regulated genes using Boolean implications, Proceedings of the National Academy of Sciences of the United States of America. 107, 5732–7. [PubMed: 20231483]
32. Stelzner M, Helmrath M, Dunn JC, Henning SJ, Houchen CW, Kuo C, Lynch J, Li L, Magness ST, Martin MG, Wong MH, Yu J & Consortium, N. I. H. I. S. C. (2012) A nomenclature for intestinal in vitro cultures, Am J Physiol Gastrointest Liver Physiol. 302, G1359–63. [PubMed: 22461030]
33. Miyoshi H & Stappenbeck TS (2013) In vitro expansion and genetic modification of gastrointestinal stem cells in spheroid culture, Nat Protoc. 8, 2471–82. [PubMed: 24232249]
34. Sato T, Vries RG, Snippert HJ, van de Wetering M, Barker N, Stange DE, van Es JH, Abo A, Kujala P, Peters PJ & Clevers H (2009) Single Lgr5 stem cells build crypt-villus structures in vitro without a mesenchymal niche, Nature. 459, 262–5. [PubMed: 19329995]
35. Sugimoto S & Sato T (2017) Establishment of 3D Intestinal Organoid Cultures from Intestinal Stem Cells, Methods Mol Biol. 1612, 97–105. [PubMed: 28634937]
36. Yu H, Hasan NM, In JG, Estes MK, Kovbasnjuk O, Zachos NC & Donowitz M (2017) The Contributions of Human Mini-Intestines to the Study of Intestinal Physiology and Pathophysiology, Annu Rev Physiol. 79, 291–312. [PubMed: 28192061]
37. Foulke-Abel J, In J, Kovbasnjuk O, Zachos NC, Ettayebi K, Blutt SE, Hyser JM, Zeng XL, Crawford SE, Broughman JR, Estes MK & Donowitz M (2014) Human enteroids as an ex-vivo model of host-pathogen interactions in the gastrointestinal tract, Exp Biol Med (Maywood). 239, 1124–34. [PubMed: 24719375]
38. Noel G, Baetz NW, Staab JF, Donowitz M, Kovbasnjuk O, Pasetti MF & Zachos NC (2017) A primary human macrophage-enteroid co-culture model to investigate mucosal gut physiology and host-pathogen interactions, Sci Rep. 7, 45270. [PubMed: 28345602]
39. Martinez-Medina M, Aldeguer X, Lopez-Siles M, Gonzalez-Huix F, Lopez-Oliu C, Dahbi G, Blanco JE, Blanco J, Garcia-Gil LJ & Darfeuille-Michaud A (2009) Molecular diversity of Escherichia coli in the human gut: new ecological evidence supporting the role of adherent-invasive E. coli (AIEC) in Crohn's disease, Inflamm Bowel Dis. 15, 872–82. [PubMed: 19235912]
40. Croxen MA, Law RJ, Scholz R, Keeney KM, Wlodarska M & Finlay BB (2013) Recent advances in understanding enteric pathogenic Escherichia coli, Clin Microbiol Rev. 26, 822–80. [PubMed: 24092857]
41. Wine E, Ossa JC, Gray-Owen SD & Sherman PM (2009) Adherent-invasive Escherichia coli, strain LF82 disrupts apical junctional complexes in polarized epithelia, BMC Microbiol. 9, 180. [PubMed: 19709415]

42. Mandell GL (1973) Interaction of intraleukocytic bacteria and antibiotics, J Clin Invest. 52, 1673–9. [PubMed: 4718959]
43. Berkes J, Viswanathan VK, Savkovic SD & Hecht G (2003) Intestinal epithelial responses to enteric pathogens: effects on the tight junction barrier, ion transport, and inflammation, Gut. 52, 439–51. [PubMed: 12584232]
44. Guttman JA & Finlay BB (2009) Tight junctions as targets of infectious agents, Biochim Biophys Acta. 1788, 832–41. [PubMed: 19059200]
45. Li Q, Zhang Q, Wang C, Li N & Li J (2008) Invasion of enteropathogenic Escherichia coli into host cells through epithelial tight junctions, FEBS J. 275, 6022–32. [PubMed: 19016848]
46. Bhinder G, Sham HP, Chan JM, Morampudi V, Jacobson K & Vallance BA (2013) The Citrobacter rodentium mouse model: studying pathogen and host contributions to infectious colitis, J Vis Exp, e50222. [PubMed: 23462619]
47. Maaser C, Housley MP, Iimura M, Smith JR, Vallance BA, Finlay BB, Schreiber JR, Varki NM, Kagnoff MF & Eckmann L (2004) Clearance of Citrobacter rodentium requires B cells but not secretory immunoglobulin A (IgA) or IgM antibodies, Infect Immun. 72, 3315–24. [PubMed: 15155635]
48. Vallance BA, Deng W, Knodler LA & Finlay BB (2002) Mice lacking T and B lymphocytes develop transient colitis and crypt hyperplasia yet suffer impaired bacterial clearance during Citrobacter rodentium infection, Infect Immun. 70, 2070–81. [PubMed: 11895973]
49. Glasser AL, Boudeau J, Barnich N, Perruchot MH, Colombel JF & Darfeuille-Michaud A (2001) Adherent invasive Escherichia coli strains from patients with Crohn's disease survive and replicate within macrophages without inducing host cell death, Infect Immun. 69, 5529–37. [PubMed: 11500426]
50. Grimm MC, Pullman WE, Bennett GM, Sullivan PJ, Pavli P & Doe WF (1995) Direct evidence of monocyte recruitment to inflammatory bowel disease mucosa, J Gastroenterol Hepatol. 10, 387–95. [PubMed: 8527703]
51. Reinecker HC, Steffen M, Witthoeft T, Pflueger I, Schreiber S, MacDermott RP & Raedler A (1993) Enhanced secretion of tumour necrosis factor-alpha, IL-6, and IL-1 beta by isolated lamina propria mononuclear cells from patients with ulcerative colitis and Crohn's disease, Clin Exp Immunol. 94, 174–81. [PubMed: 8403503]
52. Tracey KJ & Cerami A (1994) Tumor necrosis factor: a pleiotropic cytokine and therapeutic target, Annu Rev Med. 45, 491–503. [PubMed: 8198398]
53. Lu B, Rutledge BJ, Gu L, Fiorillo J, Lukacs NW, Kunkel SL, North R, Gerard C & Rollins BJ (1998) Abnormalities in monocyte recruitment and cytokine expression in monocyte chemoattractant protein 1-deficient mice, J Exp Med. 187, 601–8. [PubMed: 9463410]
54. Deshmane SL, Kremlev S, Amini S & Sawaya BE (2009) Monocyte chemoattractant protein-1 (MCP-1): an overview, J Interferon Cytokine Res. 29, 313–26. [PubMed: 19441883]
55. Murch SH, Braegger CP, Walker-Smith JA & MacDonald TT (1993) Location of tumour necrosis factor alpha by immunohistochemistry in chronic inflammatory bowel disease, Gut. 34, 1705–9. [PubMed: 8031350]
56. Hager CL & Ghannoum MA (2017) The mycobiome: Role in health and disease, and as a potential probiotic target in gastrointestinal disease, Dig Liver Dis. 49, 1171–1176. [PubMed: 28988727]
57. Caprilli R & Frieri G (2009) The dyspeptic macrophage 30 years later: an update in the pathogenesis of Crohn's disease, Dig Liver Dis. 41, 166–8. [PubMed: 19026604]
58. Baumgart M, Dogan B, Rishniw M, Weitzman G, Bosworth B, Yantiss R, Orsi RH, Wiedmann M, McDonough P, Kim SG, Berg D, Schukken Y, Scherl E & Simpson KW (2007) Culture independent analysis of ileal mucosa reveals a selective increase in invasive Escherichia coli of novel phylogeny relative to depletion of Clostridiales in Crohn's disease involving the ileum, ISME J. 1, 403–18. [PubMed: 18043660]
59. Zheng XB, Liu HS, Zhang LJ, Liu XH, Zhong XL, Zhou C, Hu T, Wu XR, Hu JC, Lian L, Deng QL, Chen YF, Ke J, He XW, Wu XJ, He XS & Lan P (2019) Engulfment and Cell Motility Protein 1 Protects Against DSS-induced Colonic Injury in Mice via Rac1 Activation, J Crohns Colitis. 13, 100–114. [PubMed: 30219846]

60. Lee CS, Penberthy KK, Wheeler KM, Juncadella IJ, Vandenabeele P, Lysiak JJ & Ravichandran KS (2016) Boosting Apoptotic Cell Clearance by Colonic Epithelial Cells Attenuates Inflammation In Vivo, Immunity. 44, 807–20. [PubMed: 27037190]

61. Carvalho FA, Barnich N, Sivignon A, Darcha C, Chan CH, Stanners CP & Darfeuille-Michaud A (2009) Crohn's disease adherent-invasive Escherichia coli colonize and induce strong gut inflammation in transgenic mice expressing human CEACAM, J Exp Med. 206, 2179–89. [PubMed: 19737864]

62. Palmieri O, Latiano A, Salvatori E, Valvano MR, Bossa F, Latiano T, Corritore G, di Mauro L, Andriulli A & Annesec V (2010) The -A2518G polymorphism of monocyte chemoattractant protein-1 is associated with Crohn's disease, Am J Gastroenterol. 105, 1586–94. [PubMed: 20125127]

63. Gerard C & Rollins BJ (2001) Chemokines and disease, Nat Immunol. 2, 108–15. [PubMed: 11175802]

64. Nakano Y, Kasahara T, Mukaida N, Ko YC, Nakano M & Matsushima K (1994) Protection against lethal bacterial infection in mice by monocyte-chemotactic and -activating factor, Infect Immun. 62, 377–83. [PubMed: 8300198]

65. Ahluwalia JP (2012) Immunotherapy in inflammatory bowel disease, Med Clin North Am. 96, 525–44, x. [PubMed: 22703854]

66. Mahe MM, Sundaram N, Watson CL, Shroyer NF & Helmrath MA (2015) Establishment of human epithelial enteroids and colonoids from whole tissue and biopsy, J Vis Exp.

67. den Hartog G, Chattopadhyay R, Ablack A, Hall EH, Butcher LD, Bhattacharyya A, Eckmann L, Harris PR, Das S, Ernst PB & Crowe SE (2016) Regulation of Rac1 and Reactive Oxygen Species Production in Response to Infection of Gastrointestinal Epithelia, PLoS Pathog. 12, e1005382. [PubMed: 26761793]

68. Kim JJ, Shajib MS, Manocha MM & Khan WI (2012) Investigating intestinal inflammation in DSS-induced model of IBD, J Vis Exp. 2 1;(60).

69. Erben U, Loddenkemper C, Doerfel K, Spieckermann S, Haller D, Heimesaat MM, Zeitz M, Siegmund B, Kühl AA (2014) A guide to histomorphological evaluation of intestinal inflammation in mouse models. Int J Clin Exp Pathol. 7 15;7(8):4557–76. [PubMed: 25197329]

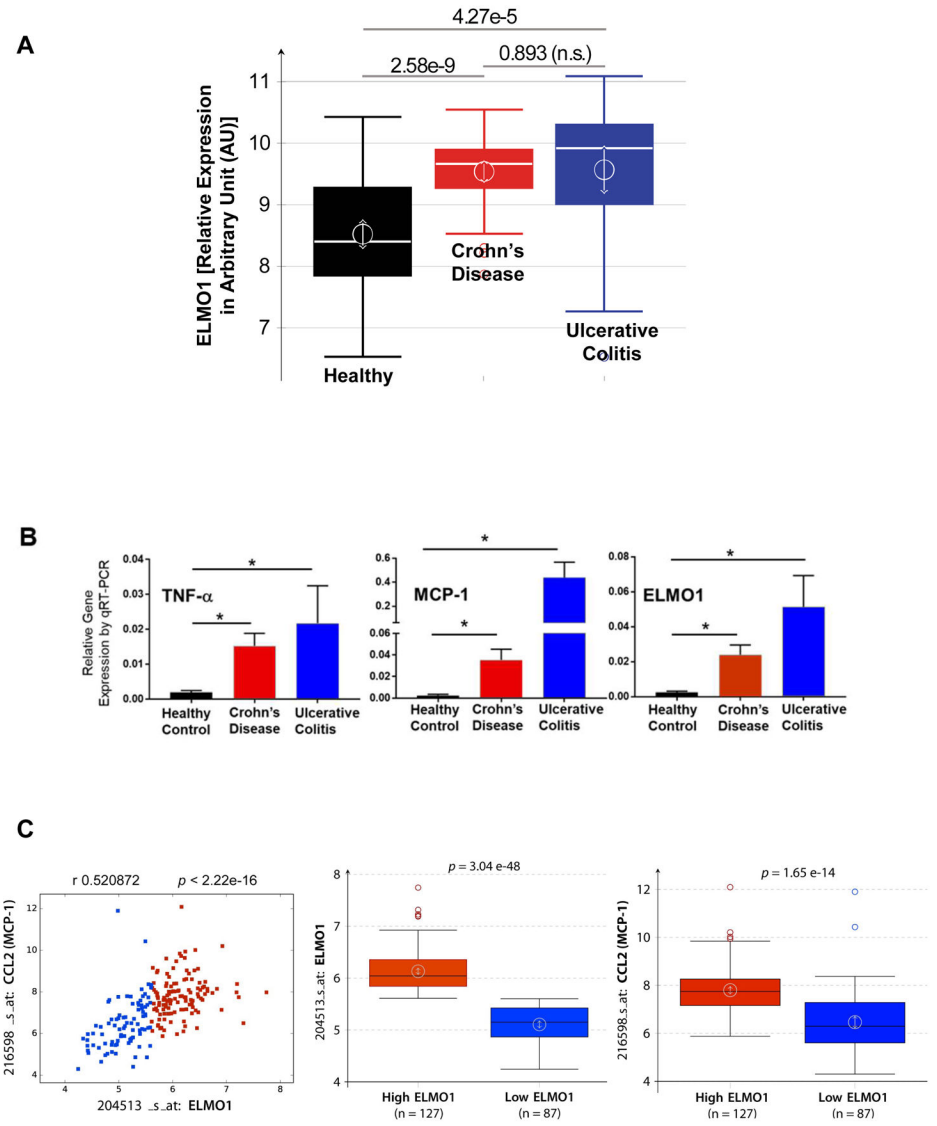

Fig. 1: ELMO1 is expressed in the gut epithelium, and its elevated expression in the gut correlates with inflammation.

(A) Gene Expression Omnibus (GEO) repository was queried for the patterns of expression of ELMO1 in publicly available cDNA microarrays [GSE83687] [28]; using the surgical specimens from 134 patients undergoing bowel resection for IBD and non-IBD controls. The ELMO1 level was determined in this cohort with 60 healthy, 42 CD (Crohn's Disease), and 32 UC (Ulcerative colitis) subjects. Data represented as mean ± SEM and *p* value was assayed by two-tailed Student's t-test. (B) Expression of ELMO1, MCP-1, and TNF-α were determined by qRT-PCR of the RNA isolated from colonic biopsies obtained from healthy controls (6 samples) and patients with CD or UC (n=8 samples/group). Data represented as mean ± SEM. * indicates p≤0.05 as assayed by two-tailed Student's t-test. (C) The association between the levels of ELMO1 and MCP-1 (*CCL2*) mRNA expression was tested in a cohort of 214 normal colon samples available in NCBI-GEO data-series (see Methods). *Left*: Graph displaying individual arrays according to the expression levels of *CCL2* and *ELMO1* in 214 normal colon tissues. Probe ID used for each gene is shown. Blue and red

indicate samples stratified into high (n = 127) vs low (n = 87) ELMO1 groups using StepMiner algorithm. *Middle*: Box plot comparing the levels of ELMO1 between high vs low ELMO1 groups. *Right*: Box plot comparing the levels of MCP-1 between high vs low ELMO1 groups. Data represented as mean ± SEM and *p* value was assayed by two-tailed Student's t-test.

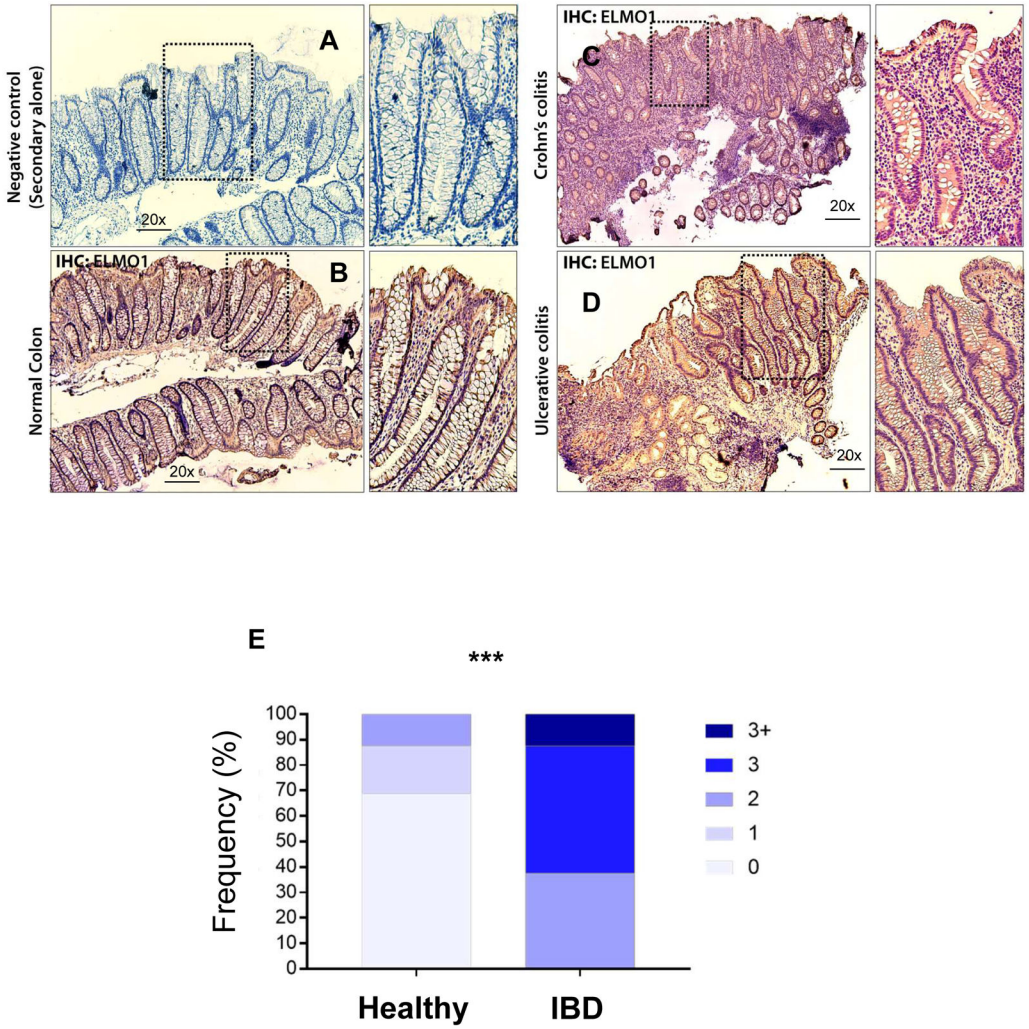

Fig. 2: ELMO1 is detected by immunohistochemistry (IHC) on biopsies

obtained from healthy controls (normal colon; left, n=5) or patients with UC or CD (right, n=8). A part of the section was stained with secondary antibody (A) that was shown as negative control and indicated the specific staining of ELMO1. A representative figure was selected from all the sections stained with ELMO1 where the patients' specimens were selected from each group of samples with healthy (B, n=5), CD (C, n=8) and UC (D, n=8) subjects. Images (A-D) displayed are representative of three independent experiments (E) The level of ELMO was determined between healthy and IBD patients' by IHC on the sections of colonic biopsies. Staining intensity was scored and compared between two groups of patients where the bar graph displays the proportion of patients in each group with varying intensities of staining; lowest as '0' and highest as '> 3+' staining (detailed in the method section). *** indicates $p \leq 0.001$ as assayed by two-tailed Student's t-test.

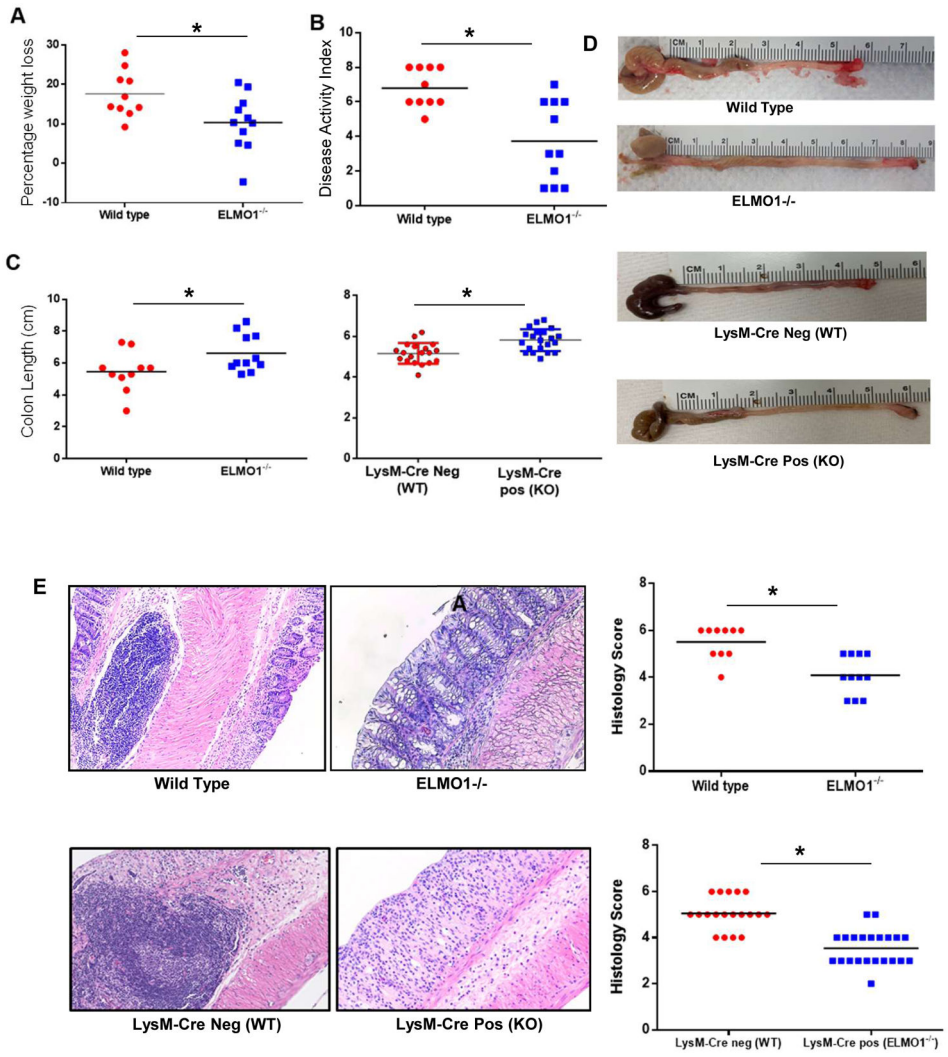

Fig. 3: ELMO1 promotes DSS-induced colitis *in vivo*.

WT mice and ELMO1$^{-/-}$ mice (global and myeloid-cell specific) were treated with DSS and the degree of colitis was assessed. (A) The substantial weight loss was monitored and depicted on day 8 in WT mice compared to the ELMO1$^{-/-}$ mice. * indicates p≤0.05 as assayed by two-tailed Student's t-test. (B) The disease activity index (DAI) was measured in which weight loss, presence of stool consistency and the presence of blood at anus were scored. * indicates p≤0.05 as assayed by two-tailed Student's t-test. (C) Colon length was measured in DSS-treated WT mice and ELMO1$^{-/-}$ mice (global) as well as with LysM cre negative WT and LysM cre positive KO mice. * indicates p≤0.05 as assayed by two-tailed Student's t-test. (D) A representative figure of the colon was shown from DSS-treated global and myeloid-cell specific ELMO1 KO mice. (E) The H&E staining and the pathology score was measured to see the degree of crypts loss, the infiltration of leukocytes in both mucosa and submucosa, and the thickening of the bowel wall from DSS-treated global and myeloid-cell specific ELMO1 KO mice. * indicates p≤0.05 as assayed by two-tailed Student's t-test.

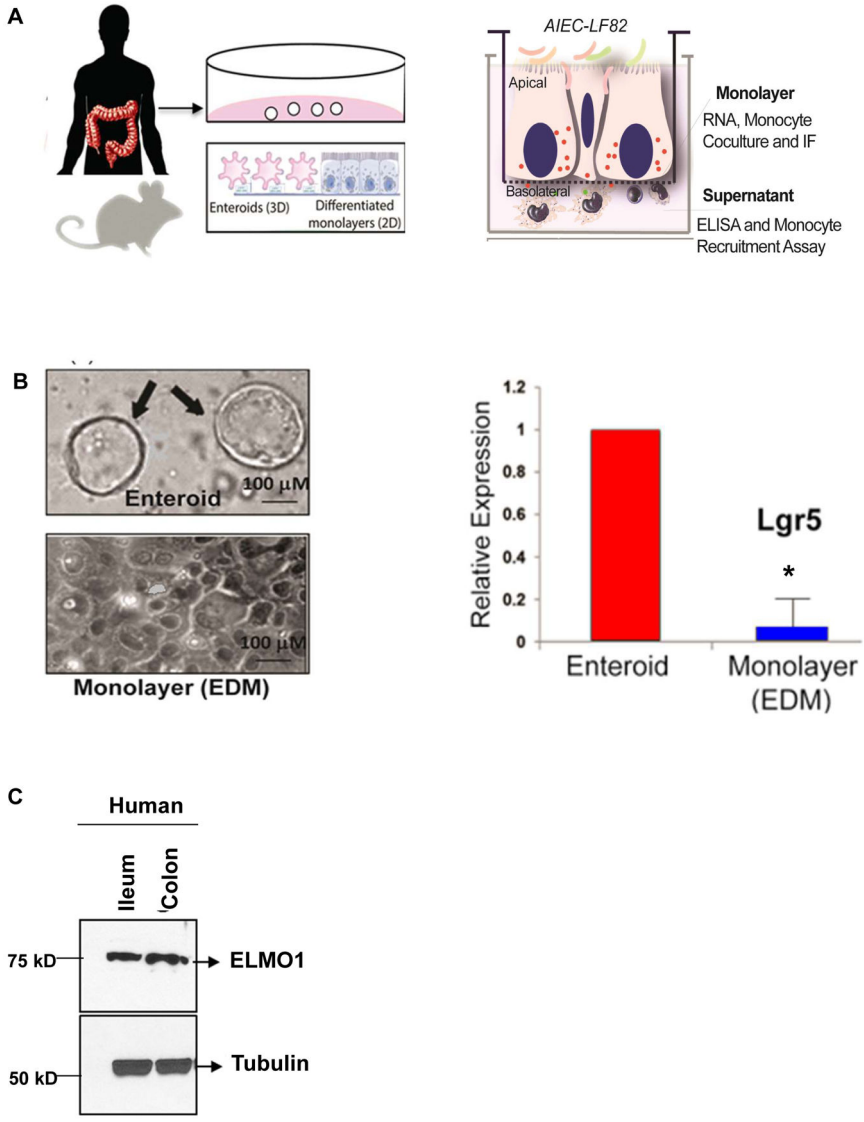

Fig. 4: Development of 3D interstinal organoid and enteroid-derived monolayers "gut-in-a-dish" model system

(A) left: Enteroids isolated from colonic biopsies that were obtained from either healthy controls or patients with CD or from the WT or ELMO1$^{-/-}$ mice. Enteroid -derived monolayers (EDM) were prepared from the enteroids via terminal differentiation (see Methods). **Right**: Schematic of experimental strategy to show the plans with the monolayer or the supernatant from the polarized EDMs. EDMs were used for RNA to test the gene expression, immunofluorescence (IF) and coculture with monocyte for recruitment assay. The supernatant was used for ELISA and monocyte recruitment assay. **(B) left:** A representative light microscopy image of spheroids (arrows) and EDMs were displayed. **Right:** The expression of Lgr5 was detected in between enteroid and EDMs to confirm the transition of stem cells to the differentiated EDMs. Data represent the mean ± SD of three separate experiments. * indicates $p \leq 0.05$ as assayed by two-tailed Student's t-test. **(C)** The expression level of ELMO1 (75 kD) was detected by immunoblotting of enteroids derived from the terminal ileum and sigmoid colon of a representative healthy subject; where α-

Tubulin was used as a loading control. We used a total of 5 healthy subjects in 5 repeated blots and out of that 5, a representative blot was selected.

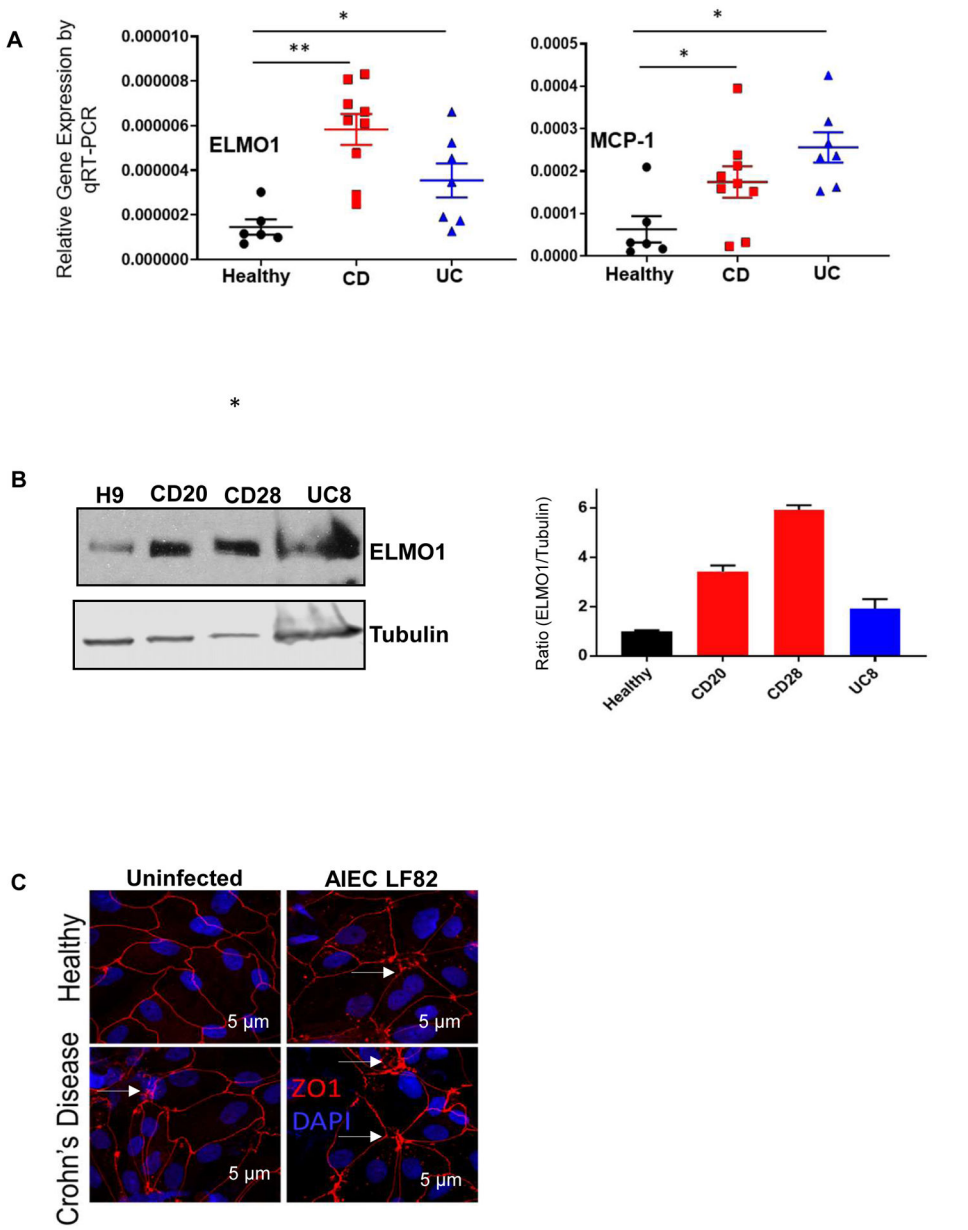

Fig 5: Integorate the role of ELMO1 in the gut epithelium

(A) The expression of ELMO1 and MCP-1 were measured in the EDMs generated from enteroid lines isolated from colonic biopsies from healthy (selected from 6 subjects), CD (9 subjects) and UC (7 subjects). The graphs display the relative expression of ELMO1 or MCP-1 in healthy, CD and UC-derived enteroids from three independent experiments and displayed as mean ± SD. * indicates $p \leq 0.05$. ** indicates $p \leq 0.01$ as assayed by two-tailed Student's t-test. **(B)** The expression level of ELMO1 was compared between healthy, CD and UC –derived enteroids. The equal loading of the lysates from colonic organoids were confirmed with Tubulin as a loading control. The densitometry plot was generated to compare the level of ELMO1 in healthy, CD and UC-derived enteroids after normalizing the intensity of ELMO1 with the loading control. The detailed information of the UC and CD

subjects were summarized in Table 2. Images displayed are representative of three independent experiments **(C)** EDMs derived from enteroids of colonic specimens of healthy and CD subjects were infected (right) or not (left) with *AIEC*-LF82 prior to fixation and stained for ZO-1 (red), a marker for TJs and nucleus (DAPI; blue). Disruptions in TJs are marked (arrowheads). In healthy EDMs, disrupted TJs are seen exclusively after infection with *AIEC*-LF82 (compare two upper images). In CD-derived EDMs, disrupted TJs were noted at baseline (lower left), almost to a similar extent as after infection with *AIEC*-LF82 (compare two lower images). The picture was a representative figure from the EDMs of 3 healthy subjects and 3 CD patients'. Images were acquired using Confocal microscope with a Plan APO 63x objective.

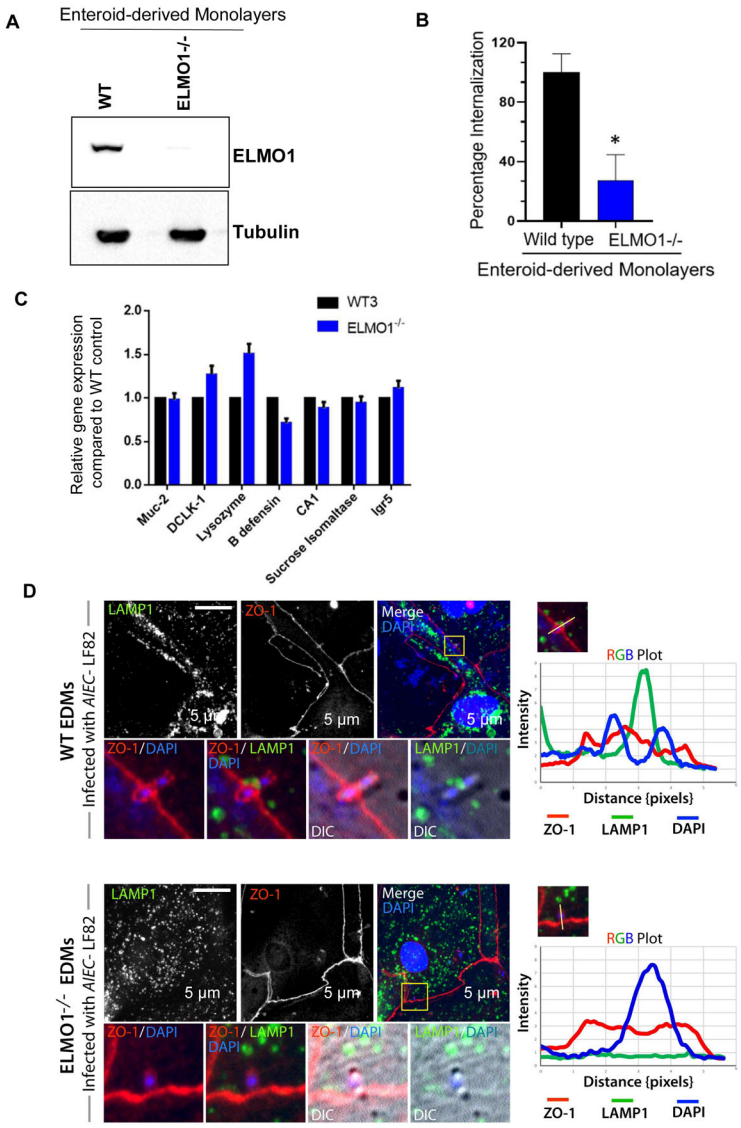

Fig. 6. The engulfment (internalization) of *AIEC*-LF82 through epithelial TJs is impaired in ELMO1$^{-/-}$ EDMs with reduced recruitment of lysosomal proteins to the sites of internalization.

(A) Expression of ELMO1 protein was assessed by immunoblotting in enteroids isolated from colons of WT and ELMO1$^{-/-}$ mice. α-Tubulin was analyzed as a loading control. Images displayed are representative of three independent experiments (B) WT and ELMO1$^{-/-}$ EDMs were infected with *AIEC*-LF82 for 6 h followed by counting the bacterial entry using gentamicin protection assay (see Methods). Bar graphs display % internalization. Data represent the mean ± SD of three separate experiments. * indicates p≤0.05 as assayed by two-tailed Student's t-test. (C) The cellular composition of WT and ELMO1$^{-/-}$ enteroids were assessed by measuring the mRNA level of different cell markers; enterocyte markers (CA1 and Sucrase isomaltase), Paneth cell markers (Lysozymes and β defensin), tuft cells markers (DCLK-1), goblet cell marker (Muc-2) and stemness marker (lgr-5). The level of expression was normalized to the housekeeping gene (18s rRNA) and then the fold change was determined by comparing with the respective control (WT) as 1. Data represent the mean ± SD of three separate experiments. * indicates p≤0.05 as assayed by two-tailed

Student's t-test. (D) WT and ELMO1$^{-/-}$ EDMs were infected with *AIEC*-LF82 as in *B*, fixed, stained with ZO1 (red), LAMP1 (green) and DAPI for nucleus, and analyzed by confocal imaging. *Left*: The maximum projection of Z-stacks of representative fields was shown. Insets in merged images represent magnified images and displayed at the bottom to zoom in at the point of bacterial entry through epithelial TJs. Lysosomes (marked by LAMP1) were aligned with the TJs (marked by ZO-1) in WT EDMs, but remain dispersed throughout the epithelial cell in ELMO1$^{-/-}$ EDMs. Lysosomes were seen in close proximity to the invading bacteria exclusively in the WT EDMs. *Right*: RGB plots show distance in pixels between the internalized bacteria (blue) and the TJs of host cells (red) and lysosomes (green). . Images were acquired using Confocal microscope with a Plan APO 63x objective.

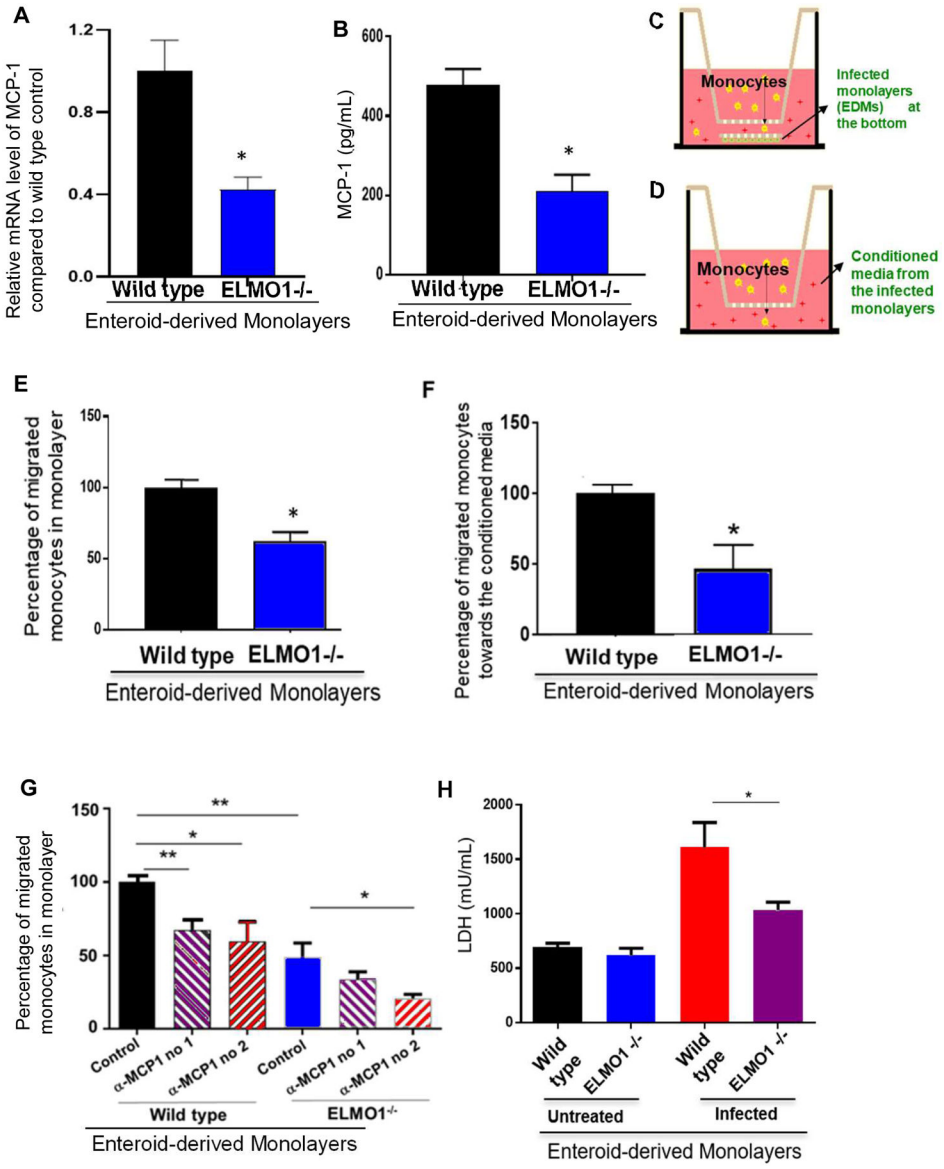

Figure 7: The induction of MCP-1 and recruitment of monocytes in response to *AIEC*-LF82 is blunted in ELMO1$^{-/-}$ EDMs; compared to WT EDMs.

(A) Levels of expression of MCP-1 was measured by qRT-PCR in EDMs derived from colonic specimens of WT and ELMO1$^{-/-}$ mice after infection with *AIEC*-LF82 for 6 h. Bar graphs display fold change in MCP-1. Data represented as mean ± SD of three separate experiments. * indicates p≤0.05 as assayed by two-tailed Student's t-test. (B) The production of MCP-1 in the supernatants of WT and ELMO1$^{-/-}$ EDMs (collected from A) was measured by ELISA. In A and B. Data represent the mean ± SD of three separate experiments. * indicates p≤0.05 as assayed by two-tailed Student's t-test. (C-D) Schematics of the EDM-monocyte coculture model used to study monocyte recruitment. Either infected EDMs (WT or ELMO1$^{-/-}$) (C) or conditioned supernatant (D) collected from infected EDMs were placed in the lower compartment where monocytes were placed in the upper chamber, separated by porous inserts of Transwell™ (see Methods). The number of

monocytes that migrated from the upper to the lower chamber by 16 h was counted. (E-F) Bar graphs display monocyte migration towards infected EDMs (E) or conditioned media (F) plotted as a percent (%) normalized to that seen when using supernatant from WT EDMs. Data represented as mean ± SD of three separate experiments. * indicates $p \leq 0.05$ as assayed by two-tailed Student's t-test. (G) The effect of MCP1 blocking was tested in the monocyte recruitment assay using the EDMs from WT and ELMO1$^{-/-}$ mice (either untreated or infected with *AIEC*-LF82 for 6 h). The conditioned supernatant was cocultured with monocytes in the presence or absence of two different MCP-1 blocking antibody (see methods). The number of monocytes that migrated from the upper to the lower chamber by 16 h was counted. Bar graphs display the percentage of monocyte migration measured in presence of control antibody or MCP-1 blocking antibodies (5 μg/ml, 1: Thermo-scientific, 2: Novus) in WT and ELMO1$^{-/-}$ EDMs, where WT EDMs with control antibody was taken as 100%. Data represented as mean ± SD of three separate experiments. * indicates $p \leq 0.05$, ** indicates $p \leq 0.01$ as assayed by two-tailed Student's t-test (H) LDH assay was performed with all the EDMs either untreated or infected with *AIEC*-LF82 collected from experiments (A-B and E). Data represented as mean ± SD of three separate experiments. * indicates $p \leq 0.05$ as assayed by two-tailed Student's t-test.

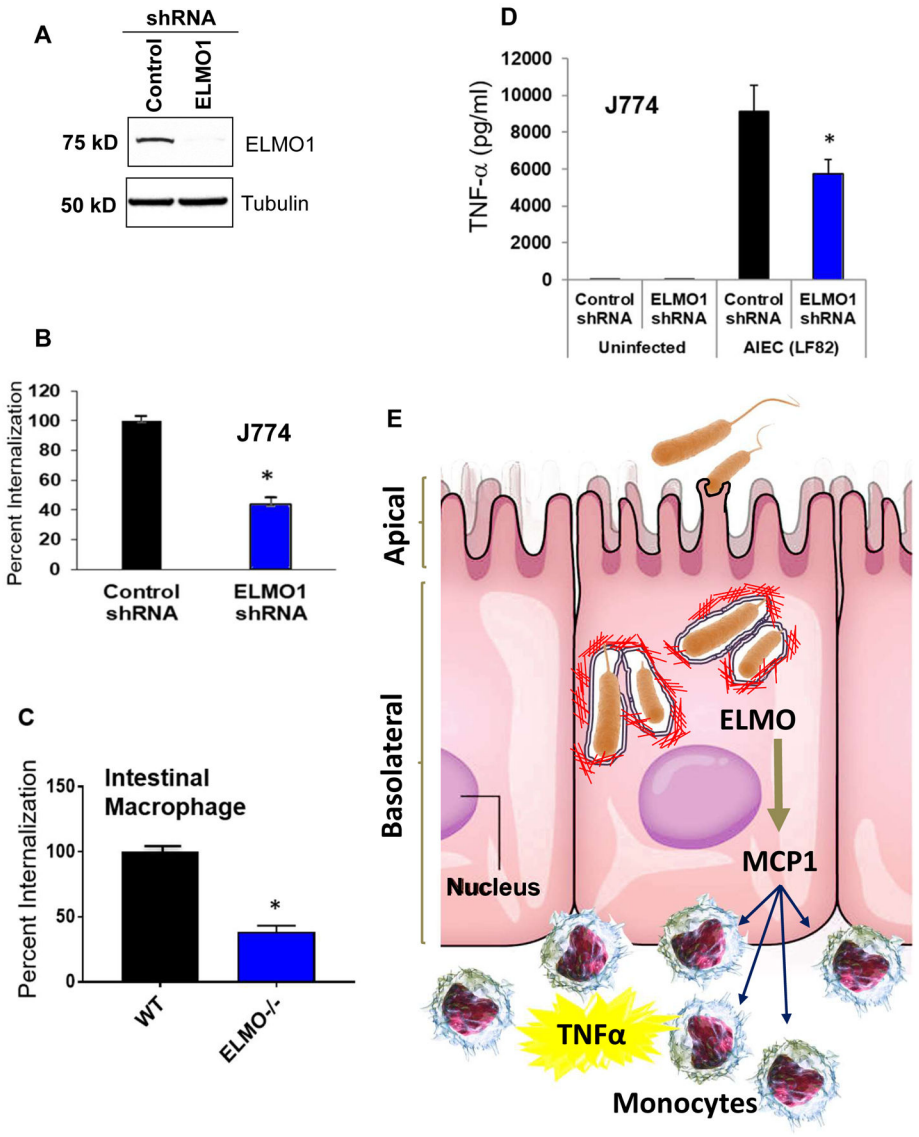

Fig. 8: Compared to WT macrophages, ELMO1-deficient macrophages display impairment in the engulfment of *AIEC*-LF82 and induction of TNF-α.

(A) The downregulation of ELMO1 in ELMO1 shRNA cell was compared to control shRNA cells by performing the Western blot of cell lysates with ELMO1 antibody and the lower panel was used for loading control with α-Tubulin. The representative blot was shown from three independent experiments. (B) Internalization of *AIEC*-LF82 in control (Control shRNA) and ELMO1-depleted (ELMO1 shRNA) J774 cells was assessed using a gentamicin protection assay as in 3*B*. Bar graphs display % internalization after 1 h of infection where control shRNA has taken as 100. Data represent mean ± SD of three separate experiments, * indicates $p \leq 0.05$ as assayed by two-tailed Student's t-test. (C) The intestinal macrophages isolated from wild type (WT) and ELMO1$^{-/-}$ mice were infected with *AIEC*-LF82 for 1 h at 37°C and bacterial internalization was measured by the gentamicin protection assay (as done in B). The average number of internalized bacteria (mean ± SD) was calculated and represented as % internalization where WT has taken as

100. * indicates p≤0.05 as assayed by two-tailed Student's t-test. (D) TNF-α produced by *AIEC*-LF82-infected J774 cells in A were analyzed by ELISA. Data represented as mean ± SD of three separate experiments. * indicates p≤0.05 as assayed by two-tailed Student's t-test. (E) Schematic summarizing the role of ELMO1 in coordinating inflammation first in non-phagocytic (epithelial) and subsequently in phagocytic (monocytes) cells of the gut. Epithelial ELMO1 is essential for the engulfment of invasive pathogens like *AIEC*-LF82 and for the induction of MCP-1 in response to such invasion. MCP-1 produced by the epithelium triggers the recruitment of monocytes, facilitating their recruitment to the site of infection. Once recruited, ELMO1 in monocytes is essential for the engulfment and clearance of invasive bacteria and for the production of pro-inflammatory cytokines such as TNF-α. MCP-1 and TNF-α released from the epithelial and monocytic cells initiate a chain reaction for the recruitment and subsequent activation of other monocytes and T-cells. The resultant storm of pro-inflammatory cytokines propagates diseases characterized by chronic inflammation.

Table 1:

Details of public available dataset (GSE83687) used in the study

Dataset (cohort composition)	**Citation**	**Genes**	**Correlation Coefficient (Pearson)**	***P* value**
GSE83687 • Controls (n=60) • UC (n=32) • CD (n=42)	PMID: 28892060	CCL2 (MCP1)	0.561486	1.6948e-12
		CXCL8 (IL8)	0.504980	4.9052e-10
		TNFA	0.484849	2.9079e-09
		IL6	0.654400	< 2.22e-16

Table 2:

Details of UC and CD subjects enrolled in the study

Subject number	Disease	Gender	Age	Disease Type	Treatment information	Disease Duration (year)
UC1	UC	Female	34	Pancolitis	Adalimumab	9
UC2	UC	Male	47	Left-sided colitis	Only ASA	21
UC3	UC	Male	19	Left-sided colitis	Infliximab (just started)	3
UC7	UC	Female	35	Proctitis	Naïve	1
UC8	UC	Male	28	Left-sided colitis	Infliximab	7
UC11	UC	Male	21	Proctitis	Vedolizumab	2
UC12	UC	Male	28	Pancolitis	Infiximab	7
CD2	CD	Female	27	Ileocolonic	Remicade	2.8
CD3	CD	Male	54	Colitis	Humira	3
CD7	CD	Female	19	Ileocolonic	Ustekinumab	<1
CD11	CD	Male	39	Stricturing, ileocolonic	Adalimumab, Vedolizumab (past)	18
CD20	CD	Male	25	Ileitis	Adalimumab	1
CD24	CD	Male	27	Stricturing	Vedolizumab	5
CD27	CD	Male	60	Penetrating, colitis	Infliximab	4
CD28	CD	Female	40	colitis	Ustekinumab	28
CD30	CD	Female	71	Ileitis	Naive	18